

Revising the definition of anthropogenic heat flux from buildings: role of human activities and building storage heat flux

Yiqing Liu¹, Zhiwen Luo¹, Sue Grimmond²

¹ School of the Built Environment, University of Reading, Reading, UK

² Department of Meteorology, University of Reading, Reading, UK

Correspondence to: * Zhiwen Luo (z.luo@reading.ac.uk) and Sue Grimmond (c.s.grimmond@reading.ac.uk)

Abstract. Buildings are a major source of anthropogenic heat emissions, impacting energy use and human health in cities. The difference [in magnitude and time lag](#) between building energy consumption and building anthropogenic heat emission [magnitudes and time lag and are is](#) poorly quantified. Energy consumption (Q_{EC}) is a widely used proxy for the anthropogenic heat flux from buildings ($Q_{F,B}$). Here we revisit the latter's definition. If $Q_{F,B}$ is the heat emission to the outdoor environment from human activities within buildings, we can derive it from the changes in energy balance fluxes between occupied and unoccupied buildings. Our derivation shows the difference between Q_{EC} and $Q_{F,B}$ is attributable to a change in the storage heat flux induced by human activities (ΔS_{o-u0}) (i.e., $Q_{F,B} = Q_{EC} - \Delta S_{o-u0}$). Using building energy simulations (EnergyPlus) we calculate the energy balance fluxes for a simplified isolated building (obtaining $Q_{F,B}$, Q_{EC} , ΔS_{o-u0}) with different occupancy states. The non-negligible differences in diurnal patterns between $Q_{F,B}$ and Q_{EC} [are](#) caused by thermal storage (e.g. hourly $Q_{F,B}$ to Q_{EC} ratios vary between -2.72 and 5.13 within a year in Beijing, China). Negative $Q_{F,B}$ can occur as human activities can reduce heat emission from [a](#) building but [this is](#) associated with a large storage heat flux. Building operations (e.g., [opening](#) windows, use of [HVAC systems](#) [space heating and cooling system](#)) modify the $Q_{F,B}$ by affecting not only Q_{EC} but also the ΔS_{o-u0} diurnal profile. Air temperature and solar radiation are critical meteorological factors explaining day-to-day variability of $Q_{F,B}$. Our new approach could be used to provide data for future parameterisations of both anthropogenic heat flux and storage heat fluxes from buildings. It is evident that storage heat fluxes in cities [may-could](#) also be impacted by occupant behaviour.

1 Introduction

Human's activities that influence energy exchanges are critical to a wide variety of disciplines (e.g. meteorology, building design, geography, climatology, hydrology, engineering). As disciplines often have

29 interests in different scales, purposes and/or boundary conditions, the terminology and acceptable assumptions
30 differ. However, disciplines may provide data to each other or help improve assumptions used. In this study we
31 are concerned with the interface between meteorology, climatology and building design in urban areas.
32 To model the weather and climate in urban areas, an important additional source of energy to the environment is
33 the anthropogenic heat flux (Q_F). This is defined as the heat converted from consumption of biological,
34 chemical and electrical energy and released to the atmosphere due to human activities (Oke et al., 2017). Q_F has
35 three major sources, including metabolic (people and animals) activities ($Q_{F,M}$), transport ($Q_{F,T}$) and buildings
36 ($Q_{F,B}$) (Grimmond, 1992). It can be large relative to incoming solar radiation in summer (e.g. 43% in an area of
37 Beijing (Nie et al., 2014)) and increases air temperature in cities (e.g. (Ichinose et al., 1999; Fan and Sailor,
38 2005)), subsequently contributing to higher cooling demand for buildings (Santamouris et al., 2001; Takane et
39 al., 2019). ~~Apart from that, Q_F is also a dominant attribution of wintertime urban heat island (Biggart et al.,
40 2021). Compared to $Q_{F,M}$ and $Q_{F,T}$, the generated heat within building volume is not all directly ejected into the
41 outdoor environment. In winter Q_F can contribute to the intensity of the urban heat island (Biggart et al., 2021).
42 Not all heat generated within the building volume is directly ejected into the outdoor environment immediately
43 but subject to change in magnitude and time lag. For example, the heat generated from human activities inside
44 buildings from mechanical heating system is released initially in the indoors environment (via heating or cooling
45 application), then transported conducted into through the building fabric by conduction, allowing it to be
46 transported and eventually emitted into atmosphere through by turbulent sensible turbulent heat flux and
47 outgoing longwave radiation. In this process the net storage heat flux (ΔQ_S) of building is modified since
48 building fabric temperature is is changed by mechanical heating system with absorbing more heat from the
49 internal heat generation.~~

50 In urban areas, ΔQ_S is the net uptake or release of energy from urban volume. This term is an important
51 determinant of urban climate and is regarded as a key process in the genesis of urban heat island (Goward,
52 1981). The change in building ΔQ_S is modified when heat is released by human activities but the timing of the
53 externally emissions are impacted by the building fabric characteristics and the conduction process. ~~With As~~
54 prior studies often ~~using use~~ energy consumption (Q_{EC}) as a proxy for $Q_{F,B}$, ~~derived~~ from inventory related
55 approaches (e.g. Sailor and Lu, 2004; Iamarino et al., 2012) and building energy modelling (e.g. Heiple and
56 Sailor, 2008; Nie et al., 2014), the impact on ΔQ_S is not addressed. To qualify the 'real' $Q_{F,B}$ and change of
57 ΔQ_S , we revisit the definition of $Q_{F,B}$ and attempt to understand how human activities affect the energy balance
58 fluxes of buildings.

59 If $Q_{F,B}$ is the heat released from buildings into the atmosphere as a result of human activities inside the
60 building (including human metabolism), when the building is completely unoccupied (e.g. no operational
61 appliances, no people; such as ‘ghost cities’ in China (Shepard, 2015) or vacant in Dublin (Kelly and Scott,
62 2018); then) $Q_{F,B}$ is zero. However, heat released from the unoccupied building is non-zero as there is still heat
63 exchange between building and ambient environment (see Eq. 1 and 2), as occurs in other environments with
64 large mass, such as forests (e.g. Oliphant et al., 2004), and rocks (e.g. Wang et al., 2018). $Q_{F,B}$ differs from
65 building heat emission (BHE) (e.g., Hong et al., 2020; Ferrando et al., 2021) as the latter is the total heat flux
66 released from buildings to the ambient air ($BHE_{uo} = Q_{H,uo} + Q_{BAE,uo} + L_{\downarrow,uo[air \rightarrow boi]} - L_{\uparrow,uo[boi \rightarrow air]}$) not due
67 to human activities alone. Shortwave and longwave radiation can enter the unoccupied internal building space
68 through windows and conduction through walls. It modifies the heat stored within the building volume and the
69 temperature of the building envelope and indoor air, subsequently influencing the emission of heat via sensible
70 heat flux, outgoing longwave radiation and air exchange. But this energy leaving the unoccupied building is not
71 anthropogenic heat flux. This energy modifies the internal building volume, influencing storage heat flux and
72 the other terms of the energy balance. These are not anthropogenic heat flux when the energy leaves the
73 unoccupied building but influence the heat emissions from the building. This is consistent with radiation
74 penetrating deep into water, and similarly allowing a larger volume to be heated than soil because of convection
75 (Sellers, 1965).

76 For an occupied building, the internal heat gain arises from:
77 (1) the equivalent sources and sinks as the unoccupied buildings; but also
78 (2) the energy linked to the indoor human activities (metabolism, powered appliances and energy inputs to
79 heating or cooling).
80 These will modify each of the energy balance fluxes. Some of this additional energy is transported out of
81 buildings through indoor-outdoor ventilation exchange and/or HVAC system, immediately contributes to $Q_{F,B}$,
82 while some is stored in the building fabric, and later is released outdoors through various pathways (convection,
83 radiation, conduction) to become $Q_{F,B}$ with a time lag. Here, we will derive $Q_{F,B}$ by looking at the difference of
84 heat fluxes between occupied and unoccupied buildings.

85 If the energy balance for the building system (including the indoor air and building envelope) for an
86 unoccupied dry building (assuming latent heat is not important in this case) is:

$$87 \quad Q_{uo}^* = Q_{H,uo} + Q_{BAE,uo} + \Delta Q_{S,uo} \quad (1)$$

88 The radiation balance for an isolated unoccupied (uo) building can be expressed as:

89 $Q_{uo}^* = K_{l,uo} - K_{t,uo} + L_{l,uo} - L_{t,uo}$ (2)

90 where Q^* is the net all-wave radiation, K is the shortwave radiation incoming (↓) and outgoing (↑) to the
 91 external surfaces. The longwave (L) radiation exchanges depend on the view factors (F) between the building of
 92 interest (*boi*), the surrounding facets of other surfaces/buildings (*other b*) and the sky:

93 $L_{l,uo} = L_{l,uo(F[sky \rightarrow boi])} + L_{l,uo(F[other b \rightarrow boi])}$ (3)

94 $L_{t,uo} = L_{l,uo(F[boi \rightarrow sky])} + L_{t,uo(F[boi \rightarrow other b])}$ (4)

95 In Eq. (1), Q_H is the turbulent sensible heat flux (convection) from external surfaces to the external ambient
 96 air. Q_{BAE} is the net energy exchange from the buildings through air exchange (e.g. ventilation). When the
 97 building is sealed Q_{BAE} is 0 W m⁻², otherwise (e.g. open windows, cracks) it can be a source or sink of energy
 98 (environment ← building, or inverse). ΔQ_S is the net storage heat flux of the building volume (i.e. fabric,
 99 contents, including the air). The left-hand side (LHS) of Eq. (1) is the inputs or source of energy to the building,
 100 whereas the right-hand side (RHS) is the sink or energy dissipation outputs. With no human activities within the
 101 building and the internal heat generation from human and infrastructure activities is zero.

102 When the building is occupied (*o*) (e.g. appliances operating / **people presence**), additional terms are
 103 needed in Eq. (1) to account for the supply of energy into the building for these activities and the release of
 104 energy:

105 $Q_o^* + Q_{Internal,o} + Q_{HVAC,o} = Q_{H,o} + Q_{BAE,o} + \Delta Q_{S,o} + Q_{Waste,o}$ (5)

106 The two additional sources of energy (LHS) are:

107 (1) $Q_{Internal,o}$: energy released within the building from lighting, powered appliances and metabolism (e.g.
 108 people, pets).

109 (2) $Q_{HVAC,o}$: energy consumption in the building from heating, ventilation and air conditioning (HVAC) system.

110 As the building may emit exhaust/waste heat (e.g. via HVAC systems), there is an additional sink (RHS)

111 referred to here as $Q_{Waste,o}$. The cooling system, $Q_{Waste,o}$ will remove energy from both anthropogenic (e.g.
 112 metabolism, lighting, electrical appliance and $Q_{HVAC,o}$) and natural sources (e.g. solar radiation through
 113 windows, heat diffusion through building envelope). Thus, only the natural sources occur in both the occupied
 114 and unoccupied states. In a 'simple' occupied state, with HVAC operated only (i.e. no people or other
 115 appliances) there is a difference in the building storage heat flux because of the alternative route to transport this
 116 natural heat of the building out from additional source of energy.

117 Here Q_H only represents the convection heat transfer at building external surface (i.e. wall, roof and windows).

118 Both $Q_{Waste,o}$ and Q_{BAE} will be incorporated into the turbulent sensible heat flux by the time they reach the

119 inertial sub-layer (ISL) or constant flux layer (CFL). Hence, sensors (e.g. eddy covariance or large aperture
 120 scintillometry) located in the ISL would observe this as Q_H . The separation of these three terms is to better
 121 understand how human activities (e.g. open/closed windows, HVAC operation) influence each heat flux. Urban
 122 canopy parameterisation (UCP) can use this information about the separate sources and their roles in the urban
 123 energy balance to account for the modified fluxes by the time they reach the ISL. Additionally, it is clearer for
 124 multi-layer UCP where vertically the energy should enter.

125 To determine the impact of the occupancy (i.e. not just the physical building form) we can consider the
 126 difference between Eq. (5) and Eq. (1). If the radiation balance for the occupied case is:

$$127 \quad Q_o^* = K_{l,o} - K_{t,o} + L_{l,o} - L_{t,o} \quad (6)$$

128 We assume that the incoming and outgoing shortwave radiation remains unchanged because the reflectivity,
 129 transmissivity and absorptivity do not change by occupancy activities then:

$$130 \quad K_{l,o} = K_{l,uo}; \quad K_{t,o} = K_{t,uo}$$

131 The incoming longwave radiation is dependent on the surroundings which are independent to the building state,
 132 so:

$$133 \quad L_{l,o} = L_{l,uo}$$

134 Thus, the difference ~~of~~ in radiative fluxes between occupied and unoccupied building ($\Delta L_{t,o-uo}$) is:

$$135 \quad \Delta L_{t,o-uo} = L_{t,o} - L_{t,uo} \quad (7)$$

136 Similarly, the difference of the heat transfer through air exchange is:

$$137 \quad \Delta BAE_{o-u} = BAE_o - BAE_{uo} \quad (8)$$

138 With the additional terms in Eq. (5) and the air exchanges rates difference from the activities within the
 139 buildings, gives:

$$140 \quad \Delta B_{o-uo} = [Q_{Internal,o} + Q_{HVAC,o}] - [Q_{Waste,o} + \Delta BAE_{o-uo}] \quad (9)$$

141 As the change in surface temperature influences the sensible heat fluxes and storage heat fluxes:

$$142 \quad \Delta H_{o-u} = H_o - H_{uo} \quad (10)$$

$$143 \quad \Delta S_{o-uo} = \Delta Q_{S,o} - \Delta Q_{S,uo} \quad (11)$$

144 By combining the Eq. (1) and Eq. (5), we obtain:

$$145 \quad \Delta B_{o-uo} = \Delta L_{t,o-uo} + \Delta H_{o-uo} + \Delta S_{o-uo} \quad (12)$$

146 where the LHS accounts for the net available energy as result of human activities in indoor environments and
 147 the RHS shows that these impact the longwave radiation, turbulent sensible and storage heat fluxes (in this dry
 148 case). With rearrangement:

149 $[Q_{Internal,o} + Q_{HVAC,o}] = \Delta S_{o-u0} + [\Delta L_{t,o-u} + \Delta H_{o-u0} + \Delta BAE_{o-u} + Q_{Waste,o}]$ (13)

150 The additional energy generation associated with human activities to the whole building system (LHS) is
 151 apparent, as traditionally defined as $Q_{F,B}$ previously (Heiple and Sailor, 2008). Here because the heat release
 152 from human metabolism indoors is considerably smaller than other sources, for simplicity of analysis, we
 153 assume metabolic heat is also part of energy consumption ($Q_{EC} = Q_{Internal,o} + Q_{HVAC,o}$). Besides, some of
 154 additional energy is associated with the extra gain or release of stored heat within the building volume (ΔS_{o-u0}).
 155 The rest is the heat released to outdoor environment from building due to human activities, which is the $Q_{F,B}$
 156 based on its definition:

157 $Q_{F,B} = \Delta L_{t,o-u0} + \Delta H_{o-u0} + \Delta BAE_{o-u0} + Q_{Waste,o}$ (14)

158 Eq. (14) demonstrates the $Q_{F,B}$ is the relative heat emission at exterior building boundary between
 159 unoccupied and occupied building through longwave radiation, convection, air exchange and waste heat from
 160 any mechanical heating/cooling system. The source of $Q_{F,B}$ within the building volume gives (by combining Eq.
 161 (13) and Eq. (14):

162 $Q_{F,B} = Q_{EC} - \Delta S_{o-u0}$ (15)

163 The sources of $Q_{F,B}$ are from both energy consumption (Q_{EC}) and difference of storage heat flux (ΔS_{o-u0})
 164 between unoccupied and occupied building ($Q_{F,B}$ in this study includes part of $Q_{F,M}$ from human metabolism).
 165 In most prior studies, Whereas the second term of Eq. (15) is ignored, in most prior studies and consequently
 166 leads to a time lag and magnitude difference between $Q_{F,B}$ and Q_{EC} (Sailor, 2011). Although the storage heat
 167 flux over a year should tend to zero, over short periods (e.g. sub-daily) ΔS_{o-u0} is not zero causing time lag and
 168 magnitude difference between $Q_{F,B}$ and Q_{EC} . Therefore, estimation of $Q_{F,B}$ by differences in heat emission
 169 between occupied and unoccupied buildings can capture the impact of dynamic changes in the building storage
 170 heat flux especially at sub-annual temporal cycle.

171 In this study, the objective is to understand the temporal profile of $Q_{F,B}$, and how and why it differs from
 172 Q_{EC} at diurnal and seasonal time scales, by examining differences in energy balance fluxes between an occupied
 173 and unoccupied same building. A bBuilding energy simulation tool (EnergyPlus) is used to obtain the various
 174 energy balance fluxes from the building system.

175 2 Methods

176 2.1 Unoccupied (uo) and occupied (o) building energy simulation (BES)

177 Building energy simulation (BES) is widely used to estimate energy consumption, heat emission and heat
178 storage within a building, while allowing changes in heat fluxes due to human activities to be estimated. Here
179 we use EnergyPlus version 9.4 (DOE, 2020) to study an isolated building (i.e. without a surrounding
180 neighbourhood). The ASNI/ASHRAE standard 140 Case 900 test model (ASHRAE, 2017) is used, which is
181 developed in a software-to-software comparative tests for validating building thermal load. It is a 48 m² one-
182 story heavyweight rectangular prism with high mass fabrics (Appendix A), whose simple geometry is ideal to
183 understand the process of how human activities change the building energy balance fluxes in a theoretical study.
184 Modifications of the original building model for this study, include: windows are reduced to one (6 m² south-
185 facing) for more appropriate EnergyPlus single-sided ventilation calculations (Daish et al., 2016); and internal
186 heat gain, ventilation control strategy and HVAC system operation vary with different scenarios considered
187 (Table 1). For the simulations, the building is assumed to be located in Beijing as the climate has both hot
188 summer and cold winter conditions. Chinese Standard Weather Data (CSWD) selected to create a Typical
189 Meteorological Year (TMY) (China Meteorological Bureau et al., 2005) are used as the meteorological forcing,
190 as these data are developed for simulating building thermal load and energy use.

191 The modelling scenarios (Table 1) vary with building occupation state. Two types of unoccupied
192 (*uo*) buildings are considered. Neither have internal heat gains nor HVAC systems, but they differ based on air
193 exchange between (1) unoccupied sealed (*us*) with no infiltration or ventilation, and (2) unoccupied ventilated
194 (*uv*) with 50% of windows area kept open. The single-sided natural ventilation rate is estimated by including
195 both wind-driven ventilation rate (V_W , m³ s⁻¹) (Warren 1977):

$$196 V_W = 0.025 A_{eff} U_W \quad (16)$$

197 and the stack buoyancy-driven ventilation rate (V , m³ s⁻¹) (Warren 1977):

$$198 V_{Stack} = \frac{1}{3} A_{eff} C_d \sqrt{\frac{\Delta T H g}{T_{ave}}} \quad (17)$$

199 where A_{eff} is the effective opening area (m²), U_W is reference wind speed at the height of opening (m s⁻¹). C_d
200 is discharge coefficient (usually taken as 0.6 (Wang and Chen, 2012)), ΔT is indoor and outdoor air temperature
201 difference (°C), H is the height of opening (m), g the gravitational acceleration (m s⁻²), T_{ave} is average indoor
202 and outdoor air temperature (°C). The combined ventilation rate is (Fan et al., 2021):

$$203 V_T = \sqrt{V_W^2 + V_{Stack}^2} \quad (18)$$

204 The three occupied (*o*) building simulations assume occupant behaviour modifies internal heat generation,
 205 natural ventilation and HVAC systems (*ov*). First, *ov1* has internal heat gains ($Q_{Internal,o}$) from human
 206 metabolism, lighting and other appliances based on local building code (MOHURD, 2018), with window always
 207 open (50%, as *uv*). The internal heat gains are held constant allowing the fraction of heat in $Q_{F,B}$ and ΔQ_S to be
 208 impacted by building and climate conditions but not the diurnal variability of human heat generation.

209 Second, *ov2* considers natural ventilation based on passive cooling and thermal comfort. The window
 210 opening is controlled automatically. It is opened (50% of window area) when the indoor air temperature is
 211 higher than both outdoor air temperature and ventilation setpoint (23°C for 'warm limit' in bedroom
 212 (Oikonomou et al., 2012)). Otherwise, it is closed to reduce heat loss and keep the building warm. Third, since
 213 natural ventilation alone may not satisfy indoor thermal comfort, mixed mode ventilation with auxiliary HVAC
 214 system (e.g. Wang and Chen, 2013; Wang and Greenberg, 2015; Chen et al., 2017) is considered in *ov3*. The
 215 mechanical heating and cooling system are active when indoor temperature reaches the threshold (18°C for
 216 heating and 26°C for cooling, MOHURD, 2018). The ventilation control strategy in *ov3* is the same as *ov2*, but
 217 the EnergyPlus hybrid ventilation manager (DOE, 2020) turns the HVAC off when natural ventilation is active
 218 to prevent simultaneous operation.

219 Table 1. Cases simulated differ based on building occupation state, internal heat gain ($Q_{Internal,o}$) and presence of natural
 220 ventilation and HVAC. Notation are defined in text and nomenclature

Code	Occupation state	Natural ventilation	$Q_{Internal,o}$ (W m ²)	Window open Temperature control (°C)	HVAC Heating/ cooling setpoint (°C)
us	uo	Sealed	0	N/A	N/A
uv	uo	Window always open (50%)	0	N/A	N/A
ov1	o	Window always open (50%)	11.8	N/A	N/A
ov2	o	Controlled ventilation	11.8	23	N/A
ov3	o	Mixed mode control	11.8	23	18/26

221 2.2 Determination of anthropogenic heat flux

222 The simulated hourly heat fluxes by radiation, convection, air exchange and waste heat generated from HVAC
 223 system between the isolated building and atmosphere (Table A.3) are analysed for each case (Table 2). If
 224 cooling occurs, the waste heat consists of the cooling load and electrical energy consumed by the air conditioner
 225 (Q_{HVAC}). Q_{HVAC} is predicted using a static coefficient of performance (COP) for the air conditioner, and the heat
 226 removed by an air conditioner (Q_{AC}) to the total amount of electricity consumed:

$$227 Q_{HVAC,c} = \frac{Q_{AC}}{COP} \quad (19)$$

$$228 Q_{Waste,c} = Q_{AC}(1 + COP^{-1}) \quad (20)$$

229 With a centralised heating system (as Beijing has), for simplicity we assume all energy associated with the
230 heating system is released indoors, and waste heat due to boiler efficiency and pipe heat loss are not considered:

$$231 \quad Q_{HVAC,H} = Q_{HS} \quad (21)$$

$$232 \quad Q_{Waste,H} = 0 \quad (22)$$

233 ~~Combing these, and accumulated through timemechanical heating and cooling, the energy consumption and~~
234 ~~corresponding waste heat from HVAC system~~ gives annual values:

$$235 \quad Q_{HVAC} = Q_{HVAC,C} + Q_{HVAC,H} = \frac{Q_{AC}}{COP} + Q_{HS} \quad (23)$$

$$236 \quad Q_{Waste} = Q_{Waste,C} + Q_{Waste,H} = Q_{AC}(1 + COP^{-1}) \quad (24)$$

237 Each term in Eq. (14) is determined using an occupied (o) and unoccupied (uo) building result to determine
238 $Q_{F,B}$ and the other fluxes. The results are analysed by season (spring (March, April and May; MAM), summer
239 (JJA), autumn (SON) and winter (DJF)) using the median (50%) and interquartile range (IQR) between the 25th
240 and 75th percentiles to assess the diurnal patterns.

241 2.3 Ratio of anthropogenic heat flux to energy consumption

242 If the energy consumed within the building is rejected immediately into the atmosphere (Heiple and Sailor,
243 2008), the change in ΔQ_S is not accounted for, and therefore $Q_{F,B}$ is assumed to be only from energy
244 consumption (Q_{EC}). The variation of ΔQ_S associated with human activities is considered when using the relative
245 heat emissions in Eq. (14) and Eq. (15). We use the ratio $R = \frac{Q_{F,B}}{Q_{EC}}$ to determine the relative importance of
246 building operation modes and choice of baselines on the discrepancy between $Q_{F,B}$ and Q_{EC} .

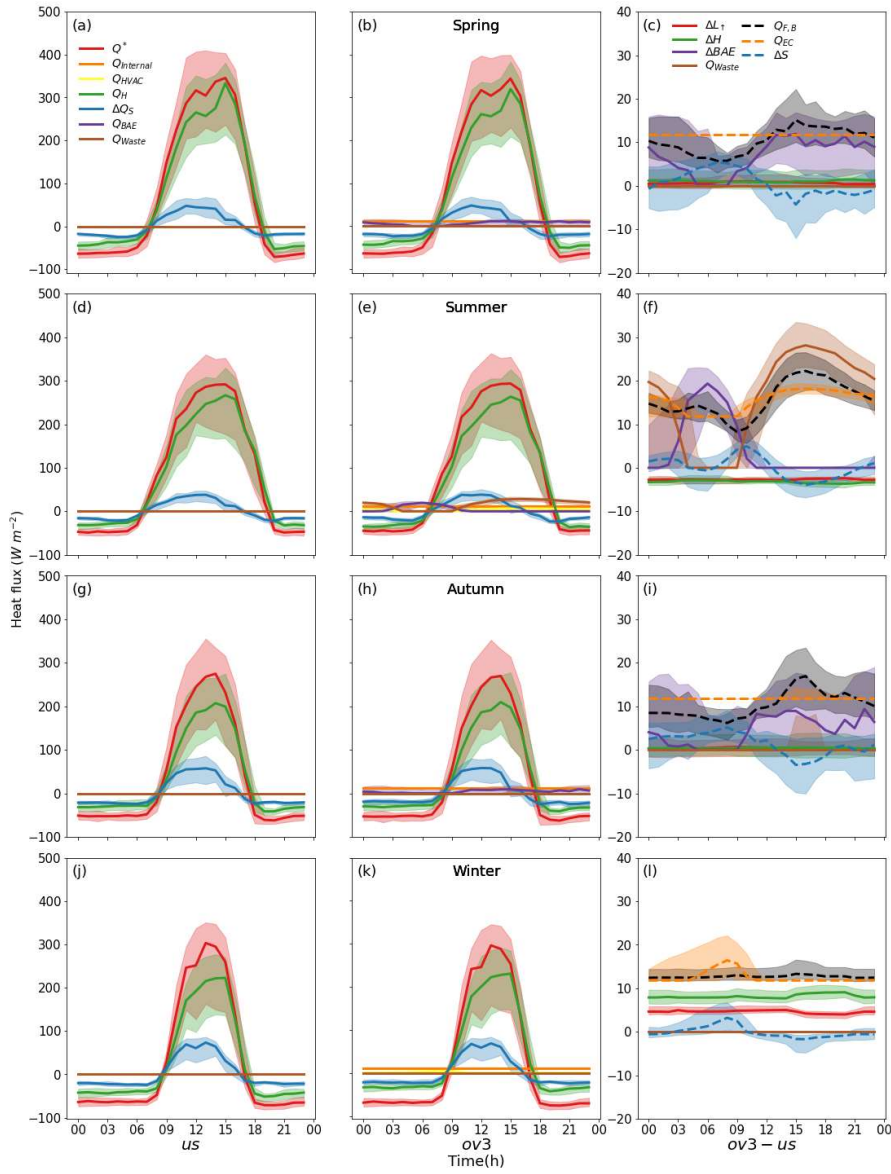
247 3 Results and discussion

248 Building energy balance fluxes vary through each day and season (Fig. 1) associated with when a building is
249 occupied and people's activities inside the building. First, we consider one case in detail - an occupied building
250 with both natural ventilation and HVAC ($ov3$, Table 31) relative to an unoccupied sealed building (us , Table 41)
251 - their difference ($ov3-us$) allows us to obtain the fluxes needed (Sect. 1).

252 As noted (Sect. 1), the shortwave and incoming longwave radiative fluxes for all cases (Table 51) are
253 assumed identical, but all other terms of the building energy balance differ. Hence, the change in outgoing
254 longwave radiation ($\Delta L_{\uparrow,o-uo}$, Fig. 1c) is equivalent to the net all-wave radiation difference (Q_{o-uo}^* , Fig. 1a-b)
255 for the occupied and unoccupied buildings. The positive sensible heat flux difference (Eq. (10), ΔH_{o-uo} , Fig. 1c)

256 and $\Delta L_{1,o-u0}$ indicate the building is warmed up by internal heat gains ($Q_{Internal,o}$) with higher exterior surface
257 temperatures. Their small magnitudes and flat patterns indicate small relative importance compared to the heat
258 exchange from ventilation differences (Eq. (8), ΔBAE_{o-u0} , Fig. 1c). The latter, not only contributes the largest
259 fraction of anthropogenic heat flux ($Q_{F,B}$, Fig. 1c), but also has a diurnal pattern consistent with $Q_{F,B}$, especially
260 during spring and autumn (Fig. 1c, i). Rarely, heat ($Q_{Waste,o}$, Fig. 1i) is emitted by the air conditioner in the
261 mid-afternoon (shading) at this time of year, but more importantly in summer (Fig. 1f) when cooling demand
262 increases.

263 $Q_{F,B}$ (Eq. (14), Fig. 1c) has four components of emitted heat, whereas energy consumption (Q_{EC} , Fig. 1c)
264 only has (in this case, constant) internal heat gains ($Q_{Internal,o} = 11.8 \text{ W m}^{-2}$, Fig. 1b, Table 61) and energy use
265 from HVAC system (Q_{HVAC} , Fig. 1b). Their difference is the storage heat flux difference (Eq. (15) ΔS_{o-u0} in Fig.
266 1c). If ΔS_{o-u0} is positive, the building acts as a heat sink and stores the extra heat generated by human activities,
267 or stored heat is released when ΔS_{o-u0} is negative. Hence, we can identify the impacts of seasonal-varying
268 human activities and building operations on the diurnal variability in ΔS_{o-u0} , Q_{EC} and $Q_{F,B}$.



269

270 Figure 1: Seasonal diurnal median (line) and inter-quantile range (IQR, shading) building heat fluxes for (a, d, g, j)
 271 unoccupied sealed (us), (b, e, h, k) occupied ventilated (ov3) building and their (c, f, i, l) difference (ov3-us) for (a-c) spring,
 272 (d-f) summer, (g-i) autumn and (j-l) winter. $Q_{F,B}$ is estimated by either heat transfer difference (solid line components):
 273 $Q_{F,B} = \Delta L_{1,o-uo} + \Delta H_{o-uo} + \Delta BAE_{o-uo} + Q_{Waste,o}$ in Eq. (14) or energy consumption and storage flux difference: $Q_{F,B} =$
 274 $Q_{EC} - \Delta S_{o-uo}$ (dash line components) in Eq. (15)

275 3.1 Impact of human activities on seasonal and diurnal variations of the fluxes

276 For the same *ov3-us* case (Table 1, Fig. 1), we consider the **temporal-diurnal** and seasonal variability of
277 the fluxes. In spring and autumn (Fig. 1a-c, g-i), natural ventilation is the dominant factor contributing to diurnal
278 variation in ΔS_{o-u0} and $Q_{F,B}$, while Q_{EC} has minimal variability. Q_{EC} is slightly larger than $Q_{Internal,o}$ because
279 of some short periods of HVAC use in the mid-afternoon (IQR shading in Fig. 1i). There is a clear diurnal cycle
280 of $Q_{F,B}$ (Fig. 1c) with the median varying between 8 W m^{-2} (07:00) and 15 W m^{-2} (15:00) relative to the constant
281 internal heat gain (11.8 W m^{-2}). The difference between $Q_{F,B}$ and Q_{EC} (ΔS_{o-u0}) is largely impacted by natural
282 ventilation. During the night and early morning with closed window, only part of the consumed energy is
283 transferred externally to the atmosphere. The rest of the heat is stored in the building fabric (positive ΔS_{o-u0}),
284 hence $Q_{F,B}$ is lower than Q_{EC} . However, when overheating may occur during the middle of the day, occupants
285 keep window opened (air conditioner is less frequently used) to cool the building down, with stored heat
286 released (negative ΔS_{o-u0}). This is consistent with the diurnal variability of ΔBAE_{o-u0} which has a minimum at
287 night (window closed) and maximum in the mid-noon (window open).

288 In summer, the **role-of-daytime** natural ventilation **at daytime** is replaced by air conditioning **as natural**
289 **ventilation alone could not maintain thermal comfort indoors**. Natural ventilation and waste heat from the air
290 conditioner ($Q_{Waste,o}$) contribute to one peak $Q_{F,B}$ at nighttime and daytime, respectively (Fig. 1f). $Q_{F,B}$ is
291 higher than Q_{EC} around these two peak periods (05:00-07:00 and 13:00-21:00). The peak $Q_{F,B}$ at night reaches
292 14 W m^{-2} (median) at 05:00, which is mainly attributed to natural ventilation when outdoor air temperature is
293 cooler than indoors. Conversely, in the afternoon when outdoor temperature is warmer, occupants 'choose'
294 mechanical cooling for achieving thermal comfort. The peak $Q_{F,B}$ is 22 W m^{-2} at 16:00, approximately 22%
295 higher than Q_{EC} . It indicates that using Q_{EC} for the anthropogenic heat flux from buildings (e.g. Heiple and
296 Sailor, 2008) may underestimate the effect of $Q_{F,B}$ on urban atmospheric processes especially during the late
297 afternoon/early evening. In addition, $Q_{F,B}$ is always smaller than $Q_{Waste,o}$ because of the negative $\Delta L_{t,o-u0}$ and
298 ΔH_{o-u0} causing a cooler exterior surface. This suggests using $Q_{Waste,o}$ as $Q_{F,B}$ (e.g. Chow et al., 2014) may
299 overestimate $Q_{F,B}$ in summer.

300 However, in winter, mechanical heating and thermal mass effect shape the temporal pattern of $Q_{F,B}$ (Fig.
301 1i). The cool outdoor air temperature before sunrise results in a substantial heating **load-supply** and peak Q_{EC}
302 (16.43 W m^{-2} for median line) at 08:00. This heat is stored in building fabric (positive ΔS_{o-u0}) and have a

303 relatively stable release through convection and longwave radiation. Therefore the diurnal profile $Q_{F,B}$ is rather
304 flatter and ΔS_{0-u} has a highly consistent temporal pattern to Q_{EC} .

305 Overall, this analysis recognizes the crucial role of ΔS_{0-u_0} in distinguishing $Q_{F,B}$ from Q_{EC} , which is highly
306 dependent on HVAC operation and natural ventilation (i.e., human activity of **opening-window opening**). These
307 two factors can rapidly increase or decrease $Q_{F,B}$ while convection and longwave radiation cannot. Whereas in
308 winter, the larger IQR (shading) of $Q_{F,B}$ than Q_{EC} indicates more day-to-day variation in $Q_{F,B}$ diurnal profile
309 than Q_{EC} . Estimates of $Q_{F,B}$ using satellite remote sensing found heat storage plays an important role in
310 moderating energy use within buildings (Yu et al., 2021). As the storage heat flux change modifies the diurnal
311 sensible heat flux pattern it modifies the surface temperature increment ($Q_{F,B}$ in remote sensing approach) and
312 hence the apparent energy consumption.

313 The diurnal profiles of ΔS_{0-u_0} are not identical between seasons as people use different actions to achieve
314 thermal comfort in different weather conditions. This suggests the $Q_{F,B}$ and Q_{EC} differences may vary between
315 climates and with cultural practices. In inventory methods the diurnal profiles may be limited (e.g. LUCY (Allen
316 et al., 2011), weekday/weekend by country) and ignore seasonal variations. However, ΔS_{0-u_0} behaviour types
317 classes may benefit from distinguishing diurnal variation for different climates.

318 3.2 Impact of different building operation modes on seasonal and diurnal variations

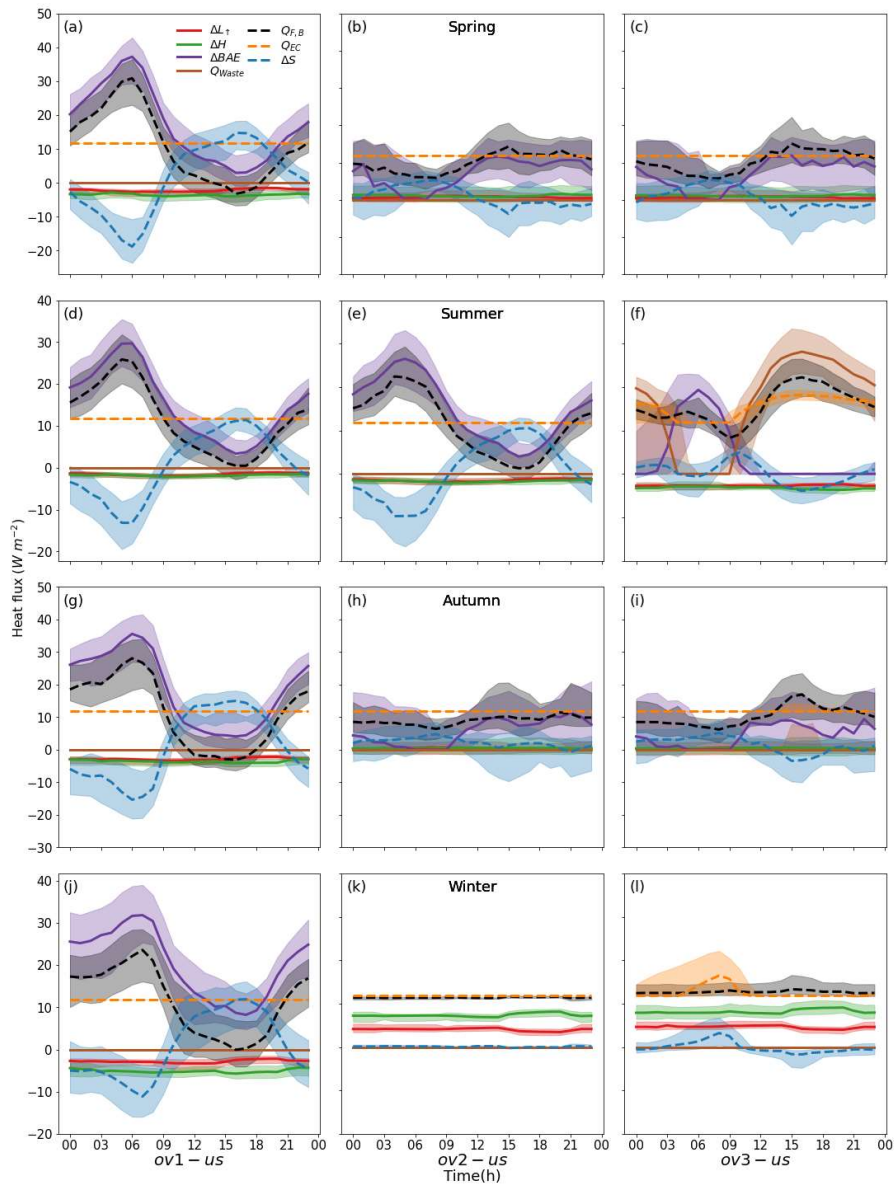
319 Fig. 2 illustrates the impact of different building operation modes ([Table 1](#): *ov1, ov2, ov3; cf. us*) on the
320 $Q_{F,B}$ diurnal profiles. It suggests the different ventilation strategies and HVAC systems do change $Q_{F,B}$ in both
321 temporal pattern and magnitude, but their impacts vary among seasons.

322 In spring and autumn, different natural ventilation control strategies completely modify the $Q_{F,B}$ diurnal
323 profile, whereas HVAC system only increases the peak $Q_{F,B}$ slightly in autumn (Fig. 2i). The distinctly different
324 (opposite) trend in diurnal $Q_{F,B}$ pattern for *ov1* cf. *ov2* or *ov3* (Fig. 2a-c, g-i) is largely explained by the diurnal
325 change of ΔBAE_{0-u_0} in the three cases. In *ov1* (window open, no control) the minimum outdoor air temperature
326 before sunrise creates the maximum indoor and outdoor air temperature difference, therefore the highest
327 ΔBAE_{0-u_0} and peak $Q_{F,B}$ at 06:00 (30 W m⁻² for the median in Fig. 2a). Whereas *ov2* and *ov3* have the window
328 closed at night and early morning to avoid overcooling, therefore the minimum $Q_{F,B}$ in the early morning
329 (07:00). As outdoor air temperature increases through the day, $Q_{F,B}$ follows the reduced ΔBAE_{0-u_0} in *ov1*,
330 whereas natural ventilation is active in *ov2* and *ov3*, leading to an increase in ΔBAE_{0-u_0} and $Q_{F,B}$. Unlike *ov2*,
331 *ov3* has a clear peak (16 W m⁻² median, Fig. 2i) at 15:00, because when natural ventilation alone cannot satisfy

332 thermal comfort and *ov3* air conditioning is activated. But their overall patterns (IQR) are very consistent,
333 indicating afternoon use of air conditioning could increase $Q_{F,B}$ magnitude but have a limited impact on other
334 parts of the diurnal pattern. Surprisingly, negative $Q_{F,B}$ occurs around 17:00 in spring (Fig. 2a), suggesting the
335 occupied building has less heat emissions than unoccupied building. Because the natural ventilation at night and
336 morning cools down the building and reduced fabric exterior surface temperature leads to a large reduction in
337 longwave radiation and convection ($\Delta L_{t,o-u0}$ and ΔH_{o-u0}) than increase in heat emission through natural
338 ventilation (ΔBAE_{o-u0}) in afternoon. And the reduced overall emissions are converted into increase in storage
339 heat flux (ΔS_{o-u0}). Negative $Q_{F,B}$ also occurs when unoccupied building is always ventilated (*uv*) and occupied
340 building is ventilated with control (*ov2* and *ov3*) in spring (e.g. Fig. B6b-c). The window is closed to avoid
341 excessive cooling at night in *ov2*. With ΔBAE_{o-u0} negative in this case, its magnitude is much larger than
342 increase in longwave radiation and convection ($\Delta L_{t,o-u0}$ and ΔH_{o-u0}). The minimum $Q_{F,B}$ frequently
343 corresponds to the peak ΔS_{o-u0} .

344 In summer, *ov2* window is open most of the time (as in *ov1*) for thermal comfort, therefore the $Q_{F,B}$ has no
345 apparent difference to *ov1*. However for *ov3*, as air conditioning runs from morning to late night and there is a
346 very different diurnal profile (cf. *ov2* and *ov1*). Air conditioner use contributes to a much larger $Q_{F,B}$ (cf. *ov2*)
347 from 12:00 to 21:00. Not only is extra energy consumed, but it also removes heat from building to the
348 atmosphere in this period. In contrast, using natural ventilation as a cooling strategy (*ov1* and *ov2*) contributes to
349 a high $Q_{F,B}$ at night and early morning but very low even negative extra heat emission in afternoon. [This implies](#)
350 [natural ventilation as passive cooling strategy not only could improve the thermal conditions indoors, but also](#)
351 [could contribute to the improvement of outdoor climate by modifying the diurnal pattern of anthropogenic heat](#)
352 [emissions \(Duan et al., 2019\).](#)

353 Consistent with results in the other seasons, different ventilation control strategies in winter cause a large
354 change in $Q_{F,B}$ profile between *ov1* and *ov2*. However, the temporal pattern of $Q_{F,B}$ (IQR) in *ov2* is quite similar
355 to *ov3* because the supplied heat from mechanical heating system does not immediately enhance $Q_{F,B}$ with
356 closed window. *ov2* is the only scenario that has similar $Q_{F,B}$ and Q_{EC} through the whole day. Comparison using
357 an unoccupied ventilated (*uv*) baseline (Fig. B.6) (cf. *uv* Fig. 2) show that although $Q_{F,B}$ profiles differ, the
358 impacts of different building operation modes are consistent when the same occupied buildings used. The
359 impact of baselines with different air exchange on $Q_{F,B}$ are analysed in Sect. 3.3.



360

361 Figure 2 : As Figure 1c, f, i, j , but comparing three different building operation types (a, d, g, j) *ov1*: window is always open

362 without control, no HVAC; (b, e, h, k) *ov2*: controlled natural ventilation for indoor thermal comfort, no HVAC; (c, f, i, l)

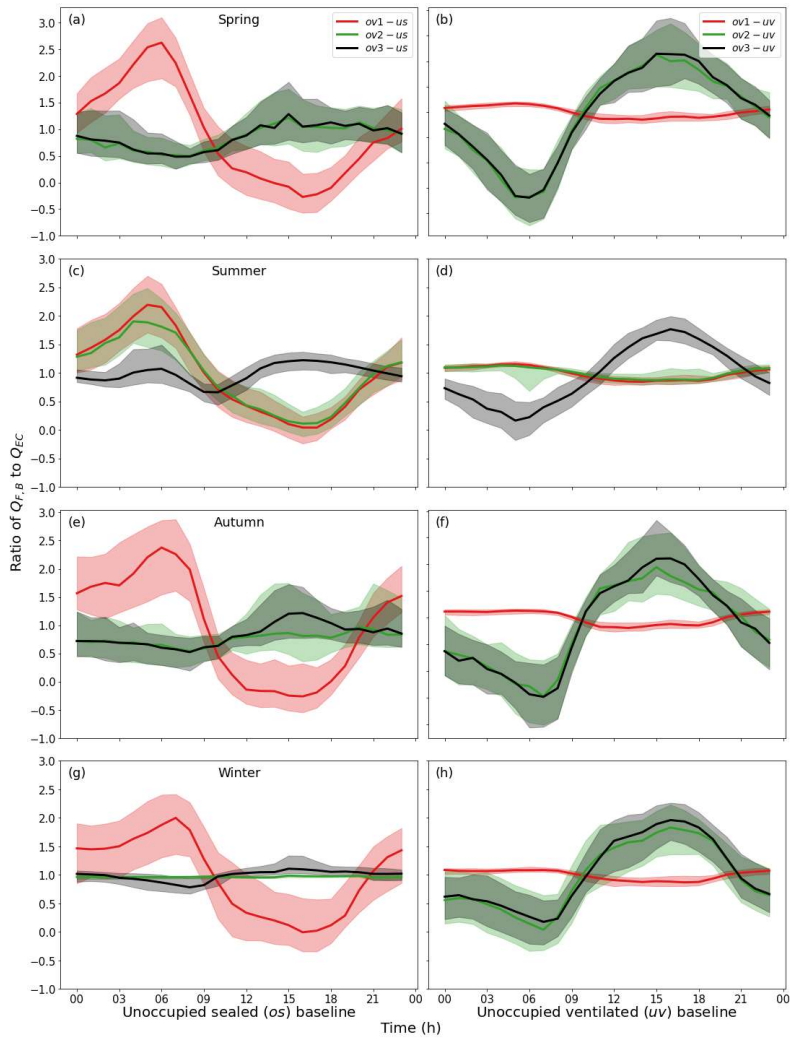
363 *ov3*: mixed mode ventilation

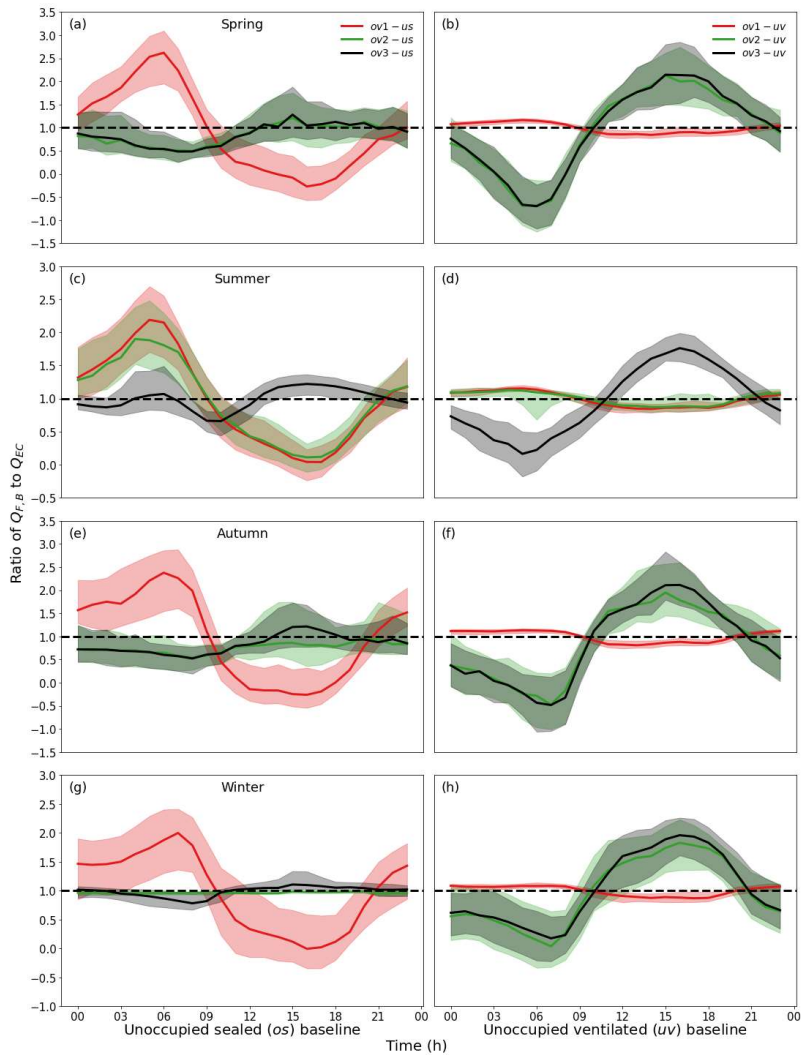
364 **3.3 Impact of unoccupied baseline chosen**

365 Here two unoccupied baselines (*us* - unoccupied sealed building, *uv* - unoccupied ventilated building with
366 uncontrolled open window) are used to assess the impact. A ratio between $Q_{F,B}$ to Q_{EC} (R) is used (Fig. 3) to
367 normalize the impact of baselines on their difference with different building operation modes. The largest
368 difference in R occurs on 23 December at 11:00, with values of 5.13 (*ov3-uv*) and -2.72 (*ov1-us*), reflecting the
369 considerable difference between $Q_{F,B}$ to Q_{EC} .

370 Two diurnal patterns of the R ratio are distinguished. When the window is always open (*ov1* in all seasons,
371 *ov2* in summer), $R > 1$ ($Q_{F,B} > Q_{EC}$) at night/early morning (22:00-08:00), reaching its maximum around
372 05:00-07:00 (near sunrise in all seasons). For the remaining periods, which are relatively warm, $R < 1$. Whereas,
373 when window opening/closing is controlled and HVAC is used for thermal comfort an almost inverse temporal
374 pattern of R occurs, with $R > 1$ during afternoon when either window is open or the air conditioner is activated.
375 The peak R occurs at 15:00 when both outdoor temperature and solar radiation are high.

376 When different unoccupied baselines are used, the temporal patterns of R are similar for all cases, but their
377 magnitudes differ significantly. R is close to 1 when window states between unoccupied and occupied buildings
378 are similar (e.g. *ov1-uv* in all seasons, *ov2-uv* in summer). Hence, greater difference occurs in heat transfer from
379 ventilation or mechanical heating/cooling between occupied and unoccupied building (i.e., larger R). Thus, the
380 baseline chosen impacts the results and require appropriate consideration for incorporating $Q_{F,B}$ into
381 atmospheric modelling.



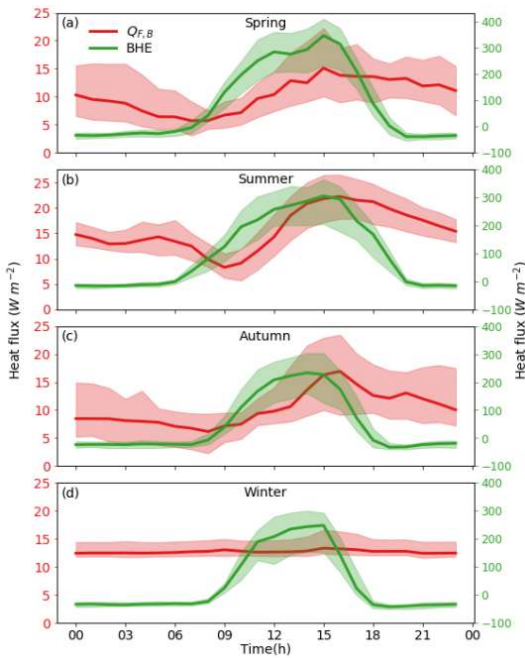


383

384 Figure 3: $Q_{F,B}$ to Q_{EC} ratio (R) median (line) and IQR (shading) for (a-b) spring, (c-d) summer, (e-f) autumn and (g-h)
 385 winter, using two unoccupied baselines: (a, c, e, g) sealed (us), and (b, d, f, h) ventilation (uv); each with three occupancy
 386 types (colour): $ov1$: Only internal heat gains are applied and window is fully open; $ov2$: Internal heat gains and natural
 387 ventilation control are applied. $ov3$: Internal heat gains, natural ventilation control and HVAC system are applied. Ratio $R=1$
 388 (Black dotted line)

389 **3.4 Comparison between $Q_{F,B}$ and building heat emission (BHM)**

390 Comparison of building heat emissions (BHE), determined using the Hong et al. (2021) approach, to $Q_{F,B}$
391 (this study) for one case (*ov3-us*) shows that the former is much larger than $Q_{F,B}$ during the day but smaller at
392 night and have different diurnal patterns (Fig. 4). Convection from the exterior envelope (Q_H , Figure 1b, e, h, k)
393 is the main contributor to BHE, therefore influences the BHE diurnal profile in each season. During the day,
394 solar radiation is large and a major control whereas $Q_{F,B}$ is relatively small and consistent but modified by
395 building-human interactions (e.g., opening windows, activation of mechanical heating and cooling systems). In
396 this scenario shown, natural ventilation and mechanical cooling dominate $Q_{F,B}$ in summer and shoulder season;
397 while in winter in their absence, convection and longwave radiation are more important.



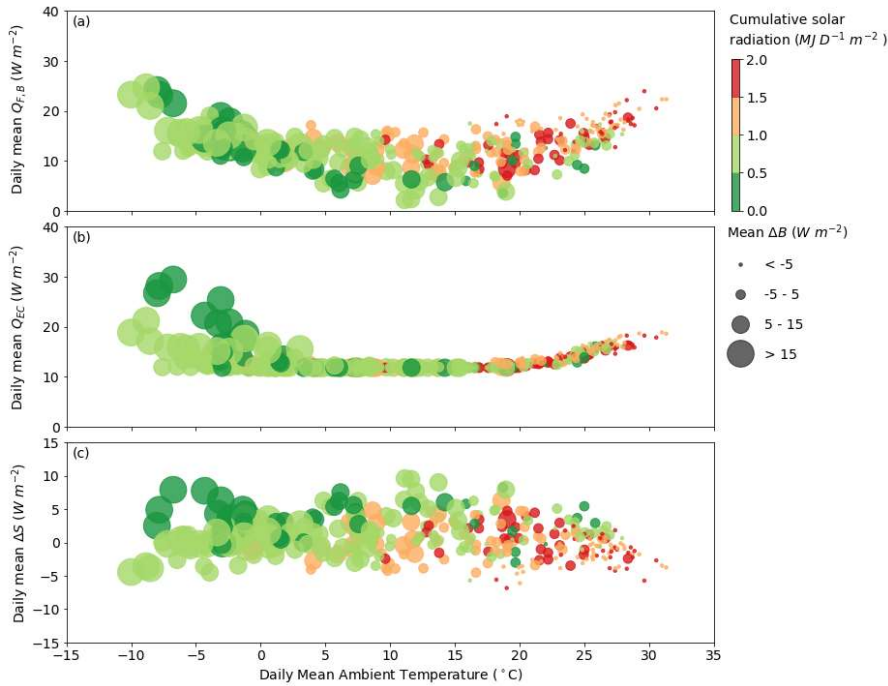
398
399 Figure 4: Comparison of seasonal diurnal $Q_{F,B}$ (*ov3-us*) and building heat emission (BHE, *ov3* in Table1) for (a) spring, (b)
400 summer, (c) autumn and (d) winter.

401 **3.4.5 Daily variation of fluxes in relation to meteorological conditions**

402 Ambient air temperature is one of the most crucial factors controlling building energy consumption (Sailor and
403 Vasireddy, 2006). Hence, it is often used to determine daily variability of Q_{EC} (e.g. Lindberg et al., 2013) and
404 the resulting monthly variations (e.g. Allen et al., 2011). By accounting for ΔS_{o-u_0} in this study, the response of

405 $Q_{F,B}$ to ambient air temperature may differ to previous studies. To examine this we use the *ov3-us* case to
406 consider the relations of daily mean (unless indicated) variables of air temperature (mean) , solar radiation (daily
407 total) and simulated available energy to the building from human activities (ΔB) with anthropogenic heat flux
408 ($Q_{F,B}$ in Fig. 4a5a), energy consumption (Q_{EC} in Fig. 4.5 b) and their difference (ΔS_{o-u_o} in Fig. 4.5 c). The overall
409 trends between $Q_{F,B}$ and Q_{EC} to ambient air temperature are consistent, with $Q_{F,B}$ and Q_{EC} smallest when
410 temperatures are between 10-15°C. This coincides with the Nicol and Humphreys'(2002) monthly balance-point
411 temperature of 12°C, which has been regarded as the equivalent ambient air temperature with the minimum
412 energy use within the building (e.g. Allen et al., 2011, Koralegedara et al., 2016). As the temperature increases
413 (decreases), Q_{EC} increases proportionally with temperature due to mechanical cooling (heating). However, in
414 contrast to Q_{EC} , $Q_{F,B}$ has a much larger variability at the same temperature caused by a large range of ΔS_{o-u_o} (-
415 7.7 to 9.0 W m⁻²), which is highly dependent on human activities on diurnal scale (Sect. 3.1)

416 To understand the large daily variability of ΔS_{o-u_o} , we use ΔB (net available energy from human activities
417 in buildings in Eq. 9) to indicate the effect of human activities (heat addition or removal) in one day. Higher ΔB
418 (larger circles) are associated with higher ΔS_{o-u_o} at the same ambient air temperature, especially in winter (Fig.
419 4e5c). This is not unexpected as buildings will absorb more heat when extra internal energy is added into the
420 building. Inversely, negative ΔB (small circles) contributes to much more heat release from heat storage (lower
421 ΔS_{o-u_o} through either natural ventilation or mechanical cooling. The sign and magnitude of ΔB are linked to
422 daily cumulative solar radiation. At the same ambient air temperature, higher-more solar radiation indicates
423 enhances the need for larger heat removal or less heat addition to the building for thermal comfort, therefore
424 leading to a smaller ΔB and lower ΔS_{o-u_o} . Consequently, we can conclude that both ambient air temperature
425 and cumulative solar radiation are important meteorological factors to determining ΔS_{o-u_o} and $Q_{F,B}$.



426

427 Figure 45: Daily results for the *ov3-us* case stratified by daily cumulative solar radiation (colour) and daily mean available
 428 energy to the building (size) (Eq. (9) associated with human activities, with mean external air (ambient) temperature and (a)
 429 mean anthropogenic heat flux, (b) energy consumption and (c) difference in storage heat flux.

430 4 Conclusions

431 Anthropogenic heat flux from buildings ($Q_{F,B}$) is defined as the additional heat released from building into
 432 atmosphere due to human activities. It is qualitatively **and quantitatively** different to building energy
 433 consumption (Q_{EC}) in temporal pattern and magnitude as result of thermal inertia of building (Iamarino et al.,
 434 2012). However, as there is no standard to quantify ‘real’ $Q_{F,B}$ most studies use Q_{EC} as a proxy via inventory
 435 and building energy modelling approaches. This paper proposes a new method to quantify a more appropriate
 436 $Q_{F,B}$ by utilising the difference in heat fluxes between an occupied and unoccupied building (i.e. the built
 437 structure with absolutely no energy use and human metabolism). We show the difference between Q_{EC} and $Q_{F,B}$
 438 is attributable to a change in the storage heat flux induced by human activities (ΔS_{o-u_0}). $Q_{F,B}$ has four
 439 components based on its dissipation pathways, including outgoing longwave radiation, turbulent sensible heat
 440 flux (convection), heat release due to air exchange and waste heat from HVAC systems. We use one simplified

441 case study in Beijing to demonstrate the analysis using building energy simulations to quantify the temporal
442 difference between Q_{EC} and $Q_{F,B}$ and understand the relative importance of building operations for thermal
443 comfort and meteorological condition on $Q_{F,B}$. The key conclusions are:

- 444 • Hourly ratios between $Q_{F,B}$ and Q_{EC} can differ between -2.72 and 5.13 because of differences in
445 occupancy use of the building (within a year, in Beijing's climate). Individual ratios frequently exceed
446 3 between 14:00 and 16:00 when controlled natural ventilation or mechanical cooling is activated in
447 shoulder season). Thus, the definitions differences are large.
- 448 • Natural ventilation (ΔBAE_{o-u0}) or HVAC operation ($Q_{Waste,o}$ for cooling and Q_{HVAC} for heating) are
449 two predominant contributors to the storage heat flux. Hence, different building operations to control
450 thermal comfort determine the diurnal profile of $Q_{F,B}$ by affecting not only Q_{EC} but also ΔS_{o-u0} .
- 451 • The day-to-day variation of $Q_{F,B}$ diurnal profile is broader than that of Q_{EC} .
- 452 • Diurnal profile of ΔS_{o-u0} varies with season as occupants modify their behaviours and the interaction
453 with buildings to achieve thermal comfort (e.g. cooling in summer and heating in winter), indicating
454 differences between $Q_{F,B}$ and Q_{EC} will vary with both climate and cultural norms.
- 455 • $Q_{F,B}$ is sensitive to the unoccupied baseline chosen (here two are analysed unoccupied sealed vs
456 unoccupied ventilated). An 'unoccupied baseline' needs to be integrated into urban climate modelling
457 in the future.
- 458 • Daily mean temperature only accounts for the day-to-day variability in Q_{EC} rather than ΔS_{o-u0} . Both
459 ambient air temperature and cumulative solar radiation are important meteorological factors to
460 determine ΔS_{o-u0} and $Q_{F,B}$.

461 Our new approach should be used to provide data for future parameterisations of both anthropogenic heat
462 flux from buildings and storage heat fluxes for urban weather and climate modelling. ~~We conclude that storage~~
463 ~~heat fluxes in cities could also be modified by occupant behaviour. We conclude that storage heat fluxes in cities~~
464 ~~is also being modified by occupant behaviour, particularly by natural ventilation and mechanical cooling. It is~~
465 ~~expected that the diurnal variation of ΔS_{o-u0} will vary with operation schedules for different building uses (e.g.~~
466 ~~residential vs. commercial buildings). Given the release of stored heat is critical influence on the nocturnal~~
467 ~~canopy layer urban heat island (CL-UHI), the impact of different HVAC operations on nocturnal UHI should be~~
468 ~~explored further. This is an important factor to determine diurnal pattern of $Q_{F,B}$ in the shoulder season and can~~
469 ~~be expressed more accurately. However, in different climates and with different social cultural practices the~~

470 periods most influenced will change. Further studies are being conducted to explore the impacts of these, while
471 also addressing feedbacks at the neighbourhood scale.

472 For developers of urban canopy parameterisations (UCP) there are several considerations because of
473 computational efficiencies essential for undertaking weather and climate modelling: (1) human activities within
474 building are modifying both the storage heat flux and the anthropogenic heat flux; (2) assuming within an UCP
475 that a 'simple' building energy model (BEM) (cf. a full building energy simulation scheme such as EnergyPlus)
476 will require some human activities to be simplified, such as using fixed ventilation rate, instead of dynamic
477 natural ventilation depending on both outdoor weather condition and thermal comfort requirements; and (3) with
478 a multi-layer UCP the appropriate levels for the impact of these energy exchanges can be accounted for. Our
479 current research is extending this analysis to consider moisture; and exploring the role of building materials,
480 construction, other aspects of building design and external meteorology. The outcome of this work will also
481 have implications for UCP development, as can help identify what can be simplified and what are critical
482 controls in different climates and urban settings.

483 This theoretical analysis is the first step towards a quantitative understanding on how $Q_{E,B}$ differs from Q_{EC} .
484 Future work should include: (i) Expand beyond our very idealised building archetype and building operation
485 mode, to more complex real-world building types and building operations; (ii) we ignore latent heat release by
486 HVAC system, such as cooling towers, these processes need to be included; and (iii) a wider range of building
487 thermal properties should be explored. For developers of urban canopy parameterisations (UCP) there are
488 several considerations because of computational efficiencies essential for undertaking weather and climate
489 modelling: (1) human activities within building are modifying both the storage heat flux and the anthropogenic
490 heat flux; (2) assuming within an UCP that a 'simple' building energy model (BEM) (cf. a full building energy
491 simulation scheme such as EnergyPlus) will require some human activities to be simplified, such as using fixed
492 ventilation rate, instead of dynamic natural ventilation depending on both outdoor weather condition and
493 thermal comfort requirements; (3) with a multi-layer UCP the appropriate levels for the impact of these energy
494 exchanges can be accounted for; (4) after extension of our analysis to consider moisture this should also be
495 accounted for; and (5) the role of building materials, construction, other aspects of building design and external
496 meteorology can be simplified once more detailed analyses are completed (e.g. sensitivity analyses) to identify
497 what the critical controls are in different climates and urban settings.

498 **Data availability**

499 [All data are deposited at https://doi.org/10.5281/zenodo.5903303 \(Liu et al., 2022\)](https://doi.org/10.5281/zenodo.5903303)

500 **Author contributions**

501 [Conceptualisation: SG and ZL, Methods and Analysis: YL SG and ZL, First draft and visualization: YL,](#)

502 [Writing and review for submission: YL, SG and ZL Funding: SG and ZL.](#)

503 **Competing interests**

504 [The author declare that they have no conflict of interest.](#)

505 **Acknowledgements**

506 [This work is funded as part of NERC-COSMA project \(NE/S005889/1\), ERC urbisphere \(855005\) and Newton](#)

507 [Fund/Met Office CSSP China Next Generation Cities \(SG, ZL\)](#)

508

509

510

511

Formatted: Indent: First line: 0 ch

512 **Nomenclature**

A_{eff}	Effective area of windows opening (m^2)
AB_{o-uo}	Available energy to the building from human activities ($W m^{-2}$)
$ABAE_{o-uo}$	Difference of heat transfer by air exchange between building and atmosphere between occupied (o) and unoccupied (uo) building ($W m^{-2}$)
BHE	Building heat emission to ambient air ($W m^{-2}$)
ΔH_{o-uo}	Difference in Q_H between occupied (o) and unoccupied (uo) building ($W m^{-2}$)
$F_{[sky \rightarrow boi]}$	View factor from sky to building of interest
$F_{[other b \rightarrow boi]}$	View factor from other buildings to building of interest
$F_{[boi \rightarrow sky]}$	View factor from building of interest to sky
$F_{[boi \rightarrow other b]}$	View factor from building of interest to other buildings
C_d	Discharge coefficient
H	Height of windows opening (m)
K_t	Outgoing shortwave radiative flux ($W m^{-2}$)
K_l	Incoming shortwave radiative flux ($W m^{-2}$)

L_t	Outgoing longwave radiative flux ($W m^{-2}$)
L_i	Incoming longwave radiative flux ($W m^{-2}$)
$\Delta L_{t, o-uo}$	Difference in L_t between occupied (o) and unoccupied (uo) building ($W m^{-2}$)
ΔQ_S	Net storage heat flux for the building volume ($W m^{-2}$)
Q^*	Net all-wave radiative flux ($W m^{-2}$)
Q_{AC}	Sensible cooling load from air conditioning ($W m^{-2}$)
Q_{BAE}	Heat transfer by air exchange between building and atmosphere ($W m^{-2}$)
$Q_{F,B}$	Anthropogenic heat flux from building sector ($W m^{-2}$)
$Q_{F,M}$	Anthropogenic heat flux from metabolic activities ($W m^{-2}$)
$Q_{F,T}$	Anthropogenic heat flux from transport ($W m^{-2}$)
Q_H	Turbulent sensible heat flux ($W m^{-2}$)
Q_{HS}	Sensible heating load ($W m^{-2}$)
Q_{HVAC}	Energy consumption by heating ventilation and air conditioning (HVAC) system ($W m^{-2}$)
$Q_{Internal}$	Internal heat gain within the building (human metabolism, lighting and appliance) ($W m^{-2}$)
Q_{Waste}	Waste heat released to outdoor by HVAC system ($W m^{-2}$)
R	Ratio of anthropogenic heat flux from building ($Q_{F,B}$) to energy consumption (Q_{EC})
ΔS_{o-uo}	Different in storage heat flux between occupied (o) and unoccupied (uo) building ($W m^{-2}$)
T_{ave}	Average indoor and outdoor air temperature ($^{\circ}C$)
ΔT	Indoor and outdoor air temperature difference ($^{\circ}C$)
U_W	Reference wind speed at height of upstream airflow ($m s^{-1}$)
V_{Stack}	Buoyance driven ventilation rate ($m^3 s^{-1}$)
V_T	Total ventilation rate by combined wind and buoyance effect
V_W	Wind driven ventilation rate ($m^3 s^{-1}$)

513

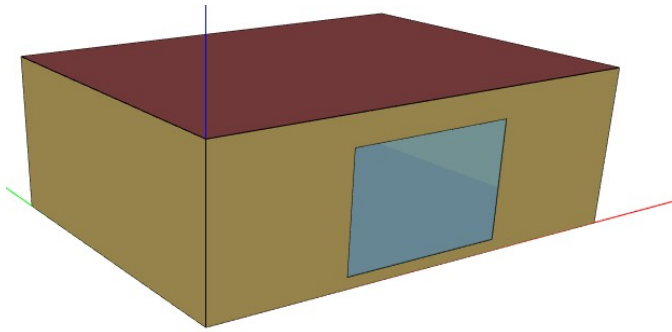
514 **Appendix A: Building energy simulation details**

515 **Table A.1:** Thermal properties of building fabric material (ASHRAE, 2017)

Opaque fabric						
Elements	Thermal conductivity ($W m^{-1}K^{-1}$)	Thickness (m)	U-value ($W m^{-2}K^{-1}$)	Thermal resistance ($m^2K^1W^{-1}$)	Density ($kg m^{-3}$)	Specific heat ($J kg^{-1}K^{-1}$)
<i>Exterior wall (inside to outdoors)</i>						
Interior surface coefficient			8.290	0.121		
Concrete block	0.510	0.100	5.100	0.196	1400	1000
Foam insulation	0.040	0.0615	0.651	1.537	10	1400
Wood siding	0.140	0.009	15.556	0.064	530	900
Exterior surface coefficient			29.300	0.034		
Overall, air to air			0.512	1.952		
<i>Floor (inside to outdoors)</i>						
Interior surface coefficient			8.290	0.121		
Concrete slab	1.130	0.08	14.125	0.071	1400	1000
Insulation	0.040	1.007	0.040	25175	0	0

Overall, air to air			0.039	25.366		
Exterior roof (inside to outdoors)						
Interior surface coefficient			8.290	0.121		
Plasterboard	0.160	0.010	16.000	0.063	950	840
Fiberglass quilt	0.040	0.1118	0.358	2.794	12	840
Roof deck	0.140	0.019	7.368	0.136	536	900
Exterior surface coefficient			29.300	0.034		
Overall, air to air			0.318	3.147		
Transparent fabric (windows)						
Number of panes					2	
Pane thickness (mm)					3.175	
Air-gap thickness (mm)					13	
Normal direct-beam transmittance through one pane					0.86156	
Thermal Conductivity of glass (W m ⁻¹ K ⁻¹)					1.06	
Exterior combined surface coefficient (W m ⁻² K ⁻¹)					21.00	
Interior combined surface coefficient (W m ⁻² K ⁻¹)					8.29	
U-value from interior air to ambient air (W m ⁻² K ⁻¹)					3.0	
Double-pane solar heat gain coefficient at normal incidence					0.789	

516 **Figure A.1:** Building geometry of ASHRAE 140 case 900 (with changed window)



517
518 **Table A.2:** Composition of internal heat gains from local building code (MOHURD, 2018). Human metabolism rate (100 W
519 p⁻¹) is typical of resting activities (e.g. sleeping, reclining, seated and standing, 72-126W p⁻¹) (ASHRAE, 2005).

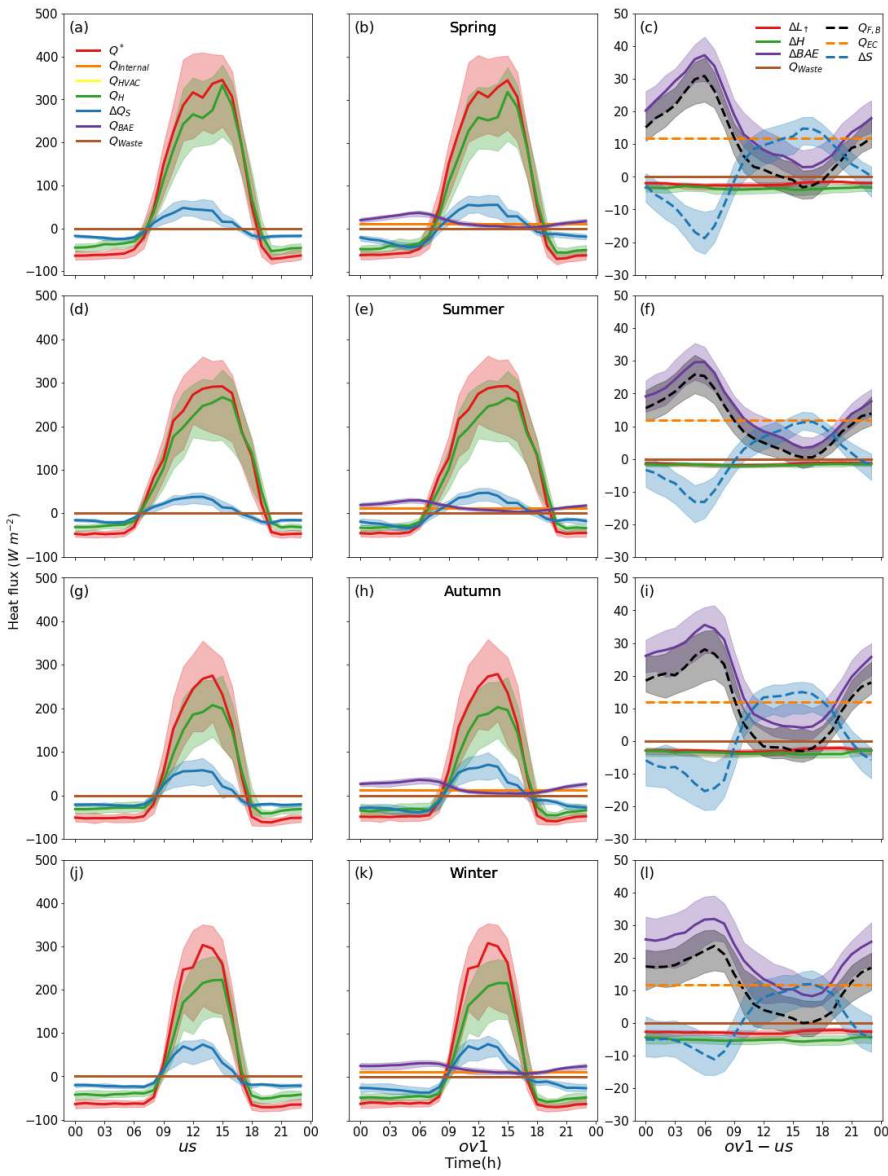
Lighting (W m ⁻²)	Equipment (W m ⁻²)	Occupancy density (p m ⁻²)
5	3.8	0.03

520 **Table A.3:** EnergyPlus output variables are used here in the following equations first. A_{Floor} – is total area of floor of the
521 building (m²)

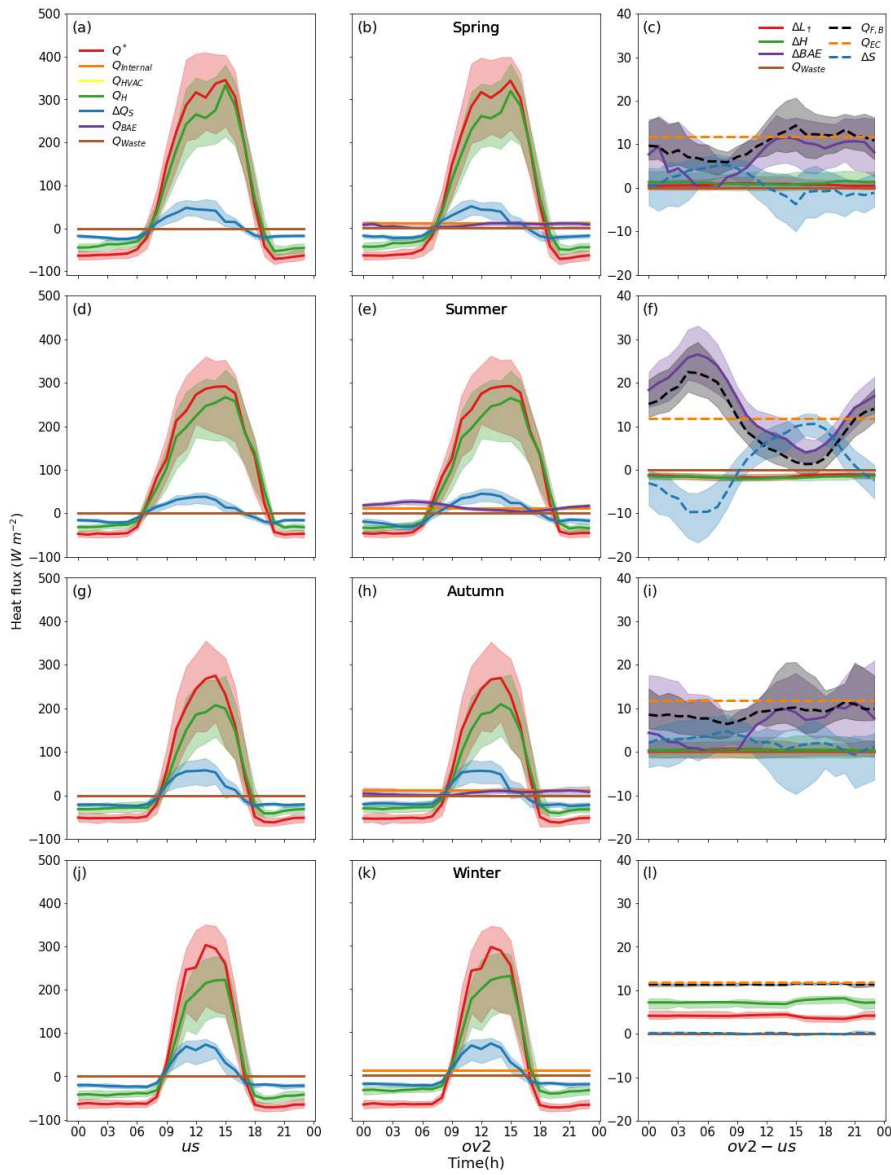
EnergyPlus output variable (Units: W)	Notation	Building volume energy balance fluxes calculated (W m ⁻²)	Equation (Units: W m ⁻²)
Outside face net thermal radiation heat gain rate	$l_{\uparrow} - l_{\downarrow}$	Net longwave radiation	$L_{\uparrow} - L_{\downarrow} = \sum_{i=1}^{N_{surface}} (l_{\uparrow} - l_{\downarrow}) / A_{floor}$
Zone total internal total heating rate	$q_{Internal}$	Internal heat gains within the whole building	$Q_{Internal} = \sum_{i=1}^{N_{zone}} q_{Internal} / A_{floor}$
Surface outside face convection heat gain rate	q_H	Turbulent sensible heat flux	$Q_H = - \sum_{i=1}^{N_{surface}} q_H / A_{floor}$
Zone air heat balance air energy storage rate	$\Delta q_{S,a}$	Net storage heat flux for the building volume	$\Delta Q_S = (\sum_{i=1}^{N_{zone}} \Delta q_{S,a} + \sum_{i=1}^{N_{surface}} \Delta q_{S,s}) / A_{floor}$
Surface heat storage rate	$\Delta q_{S,s}$		
AFN (Airflow-network) – zone exfiltration sensible heat transfer rate	Δq_{BAE}	Heat transfer by air exchange between building and atmosphere	$Q_{BAE} = \sum_{i=1}^{N_{zone}} q_{BAE} / A_{floor}$

Zone ideal loads supply air sensible heating rate	Δq_{HS}	Sensible heating load	$Q_{HS} = \sum_{i=1}^{N_{zone}} q_{HS} / A_{floor}$
Zone ideal loads supply air sensible cooling rate	Δq_{AC}	Sensible cooling load	$Q_{AC} = \sum_{i=1}^{N_{zone}} q_{AC} / A_{floor}$

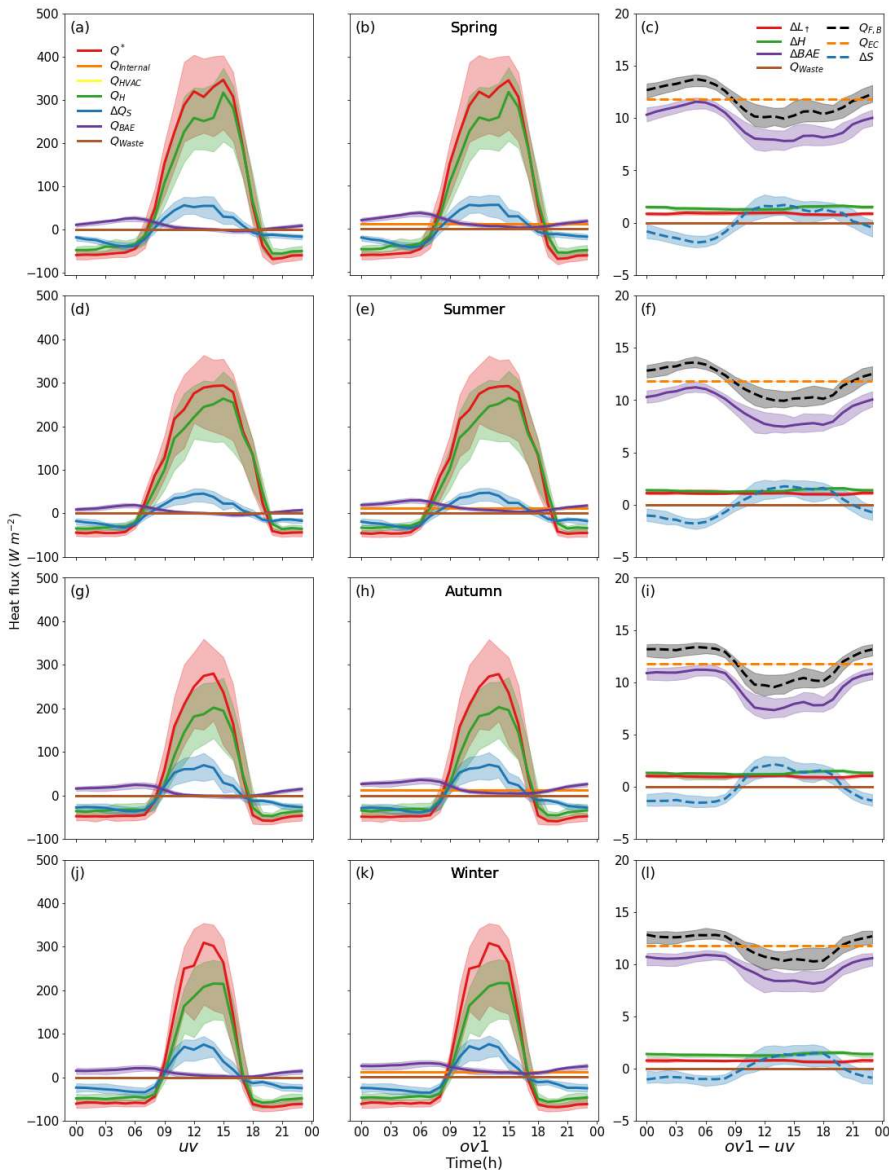
522 Appendix B: Energy balance analysis for other cases



524 Figure B1. As Figure 1, but uses *ov1* for occupied building case in (b, e, h, k) and the heat flux difference with respect to
 525 unoccupied sealed building (*ov1-us*) in (c, f, i, l)



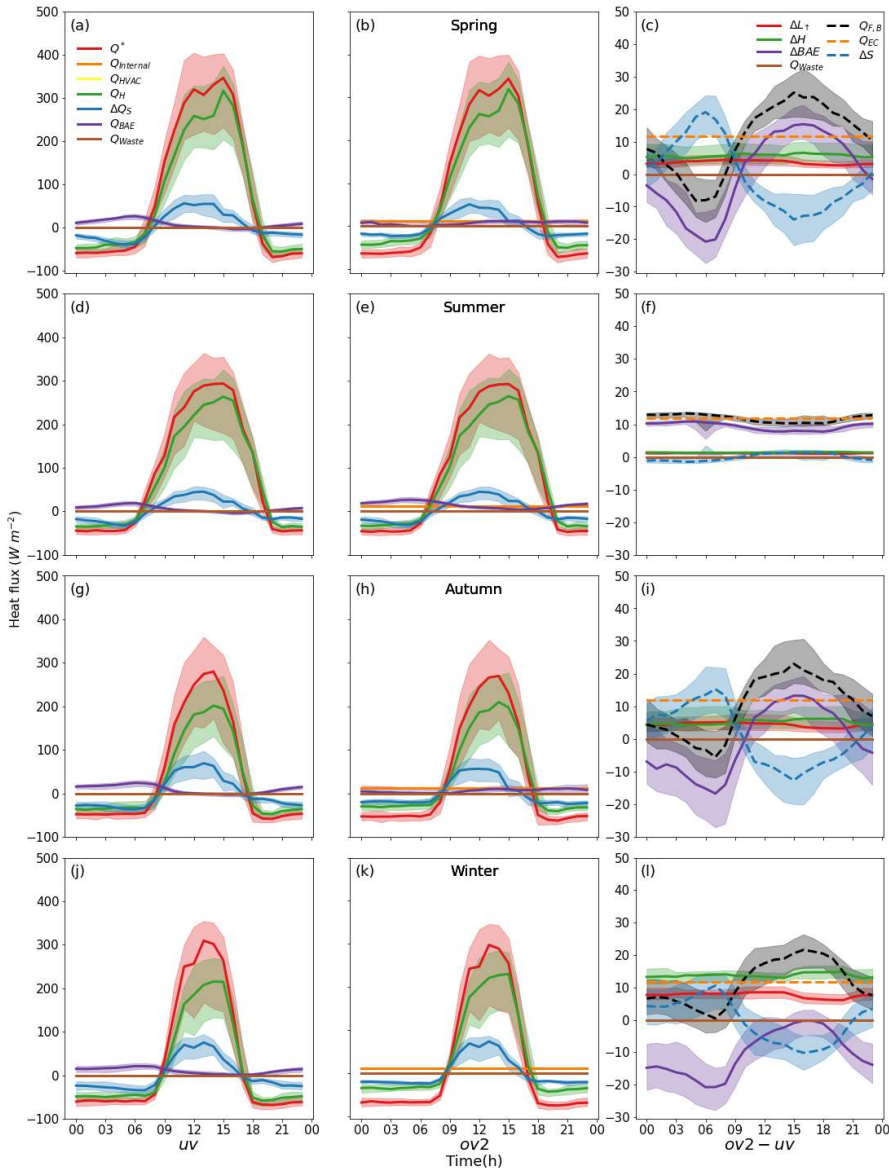
526
 527 Figure B2. As Figure B1, but uses *ov2* for occupied building case in (b, e, h, k) and the heat flux difference with respect to
 528 unoccupied sealed building (*ov2-us*) in (c, f, i, l)



529

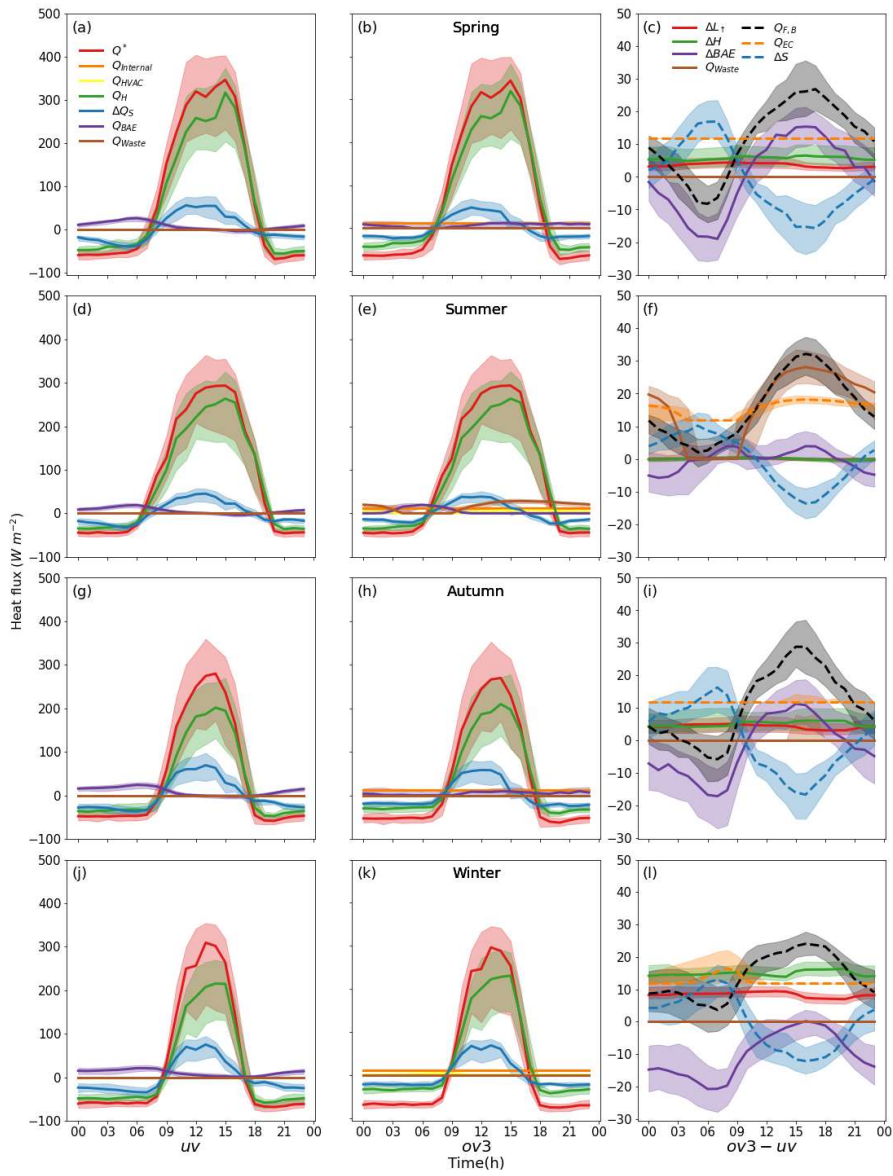
530 Figure B3. As Figure B2, but uses unoccupied ventilation baseline (a, d, g, j) and occupied building case *ov1* in (b, e, h, k)

531 and their difference (*ov1-uv*) in (c, f, i, l)



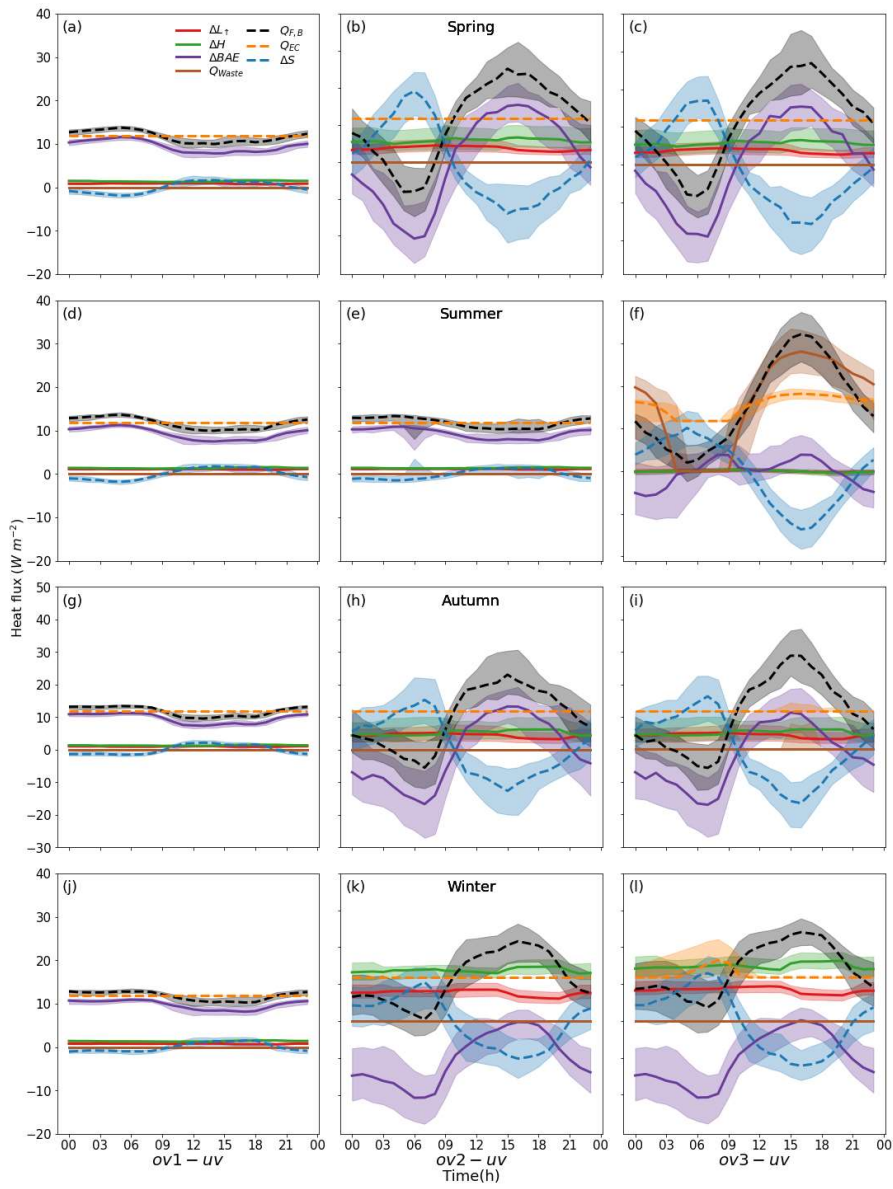
532

533 Figure B4. As Figure B3, but uses occupied building case $ov2$ in (b, e, h, k) and their difference ($ov2-uv$) in (c, f, i, l)



534

535 Figure B5. As Figure B3, but with $ov3$ in (b, e, h, k) and their difference ($ov3-uv$) in (c, f, i, l)



536

537 Figure B6. As Figure 2 but with uv as the baseline

538 **Acknowledgements**

539 [This work is funded as part of NERC-COSMA project \(NE/S005889/1\), ERC urbisphere \(855005\) and Newton](#)
540 [Fund/Met-Office CSSP China Next-Generation Cities \(SG, ZL\)](#)

541 **References**

- 542 Allen, L., Lindberg, F. and Grimmond, C. S. B.: Global to city scale urban anthropogenic heat flux: Model and
543 variability, *Int. J. Climatol.*, 31(13), 1990–2005, doi:10.1002/joc.2210, 2011.
- 544 ASHRAE: ANSI/ASHRAE Standard 140-2017 Standard method of test for the evaluation of building energy
545 analysis computer programs., 2017.
- 546 Biggart, M., Stocker, J., Doherty, R. M., Wild, O., Carruthers, D., Grimmond, S., Han, Y., Fu, P. and Kotthaus,
547 S.: Modelling spatiotemporal variations of the canopy layer urban heat island in Beijing at the neighbourhood
548 scale, *Atmos. Chem. Phys.*, 21(17), 13687–13711, doi:10.5194/acp-21-13687-2021, 2021.
- 549 Chen, X., Yang, H. and Wang, Y.: Parametric study of passive design strategies for high-rise residential
550 buildings in hot and humid climates: miscellaneous impact factors, *Renew. Sustain. Energy Rev.*, 69(January
551 2016), 442–460, doi:10.1016/j.rser.2016.11.055, 2017.
- 552 China Meteorological Bureau, Climate Information Center, Climate Data Office and Tsinghua University,
553 Department of Building Science and Technology.: China Standard Weather Data for Analyzing Building
554 Thermal Conditions, Beijing: China Building Industry Publishing House, ISBN 7-112-07273-3 (13228), 2005.
- 555 Chow, W. T. L., Salamanca, F., Georgescu, M., Mahalov, A., Milne, J. M. and Ruddell, B. L.: A multi-method
556 and multi-scale approach for estimating city-wide anthropogenic heat fluxes, *Atmos. Environ.*, 99, 64–76,
557 doi:10.1016/j.atmosenv.2014.09.053, 2014.
- 558 Daish, N. C., Carrilho da Graça, G., Linden, P. F. and Banks, D.: Impact of aperture separation on wind-driven
559 single-sided natural ventilation, *Build. Environ.*, 108, 122–134, doi:10.1016/j.buildenv.2016.08.015, 2016.
- 560 DOE.: EnergyPlus™ Version 9.4.0, <https://energyplus.net/>, 2020.
- 561 DOE.: EnergyPlus™ Version 9.4.0 Input Output Reference, 2020.
- 562 Duan, S., Luo, Z., Yang, X. and Li, Y.: The impact of building operations on urban heat/cool islands under
563 urban densification: A comparison between naturally-ventilated and air-conditioned buildings, *Appl. Energy*,
564 235(November 2018), 129–138, doi:10.1016/j.apenergy.2018.10.108, 2019.
- 565 Fan, H. and Sailor, D. J.: Modeling the impacts of anthropogenic heating on the urban climate of Philadelphia:

566 A comparison of implementations in two PBL schemes, *Atmos. Environ.*, 39(1), 73–84,
567 doi:10.1016/j.atmosenv.2004.09.031, 2005.

568 Fan, S., Davies Wykes, M. S., Lin, W. E., Jones, R. L., Robins, A. G. and Linden, P. F.: A full-scale field study
569 for evaluation of simple analytical models of cross ventilation and single-sided ventilation, *Build. Environ.*,
570 187(July 2020), 107386, doi:10.1016/j.buildenv.2020.107386, 2021.

571 Ferrando, M., Hong, T. and Causone, F.: A simulation-based assessment of technologies to reduce heat
572 emissions from buildings, *Build. Environ.*, 195(August 2020), 107772, doi:10.1016/j.buildenv.2021.107772,
573 2021.

574 Goward, S. N.: Thermal behavior of urban landscapes and the urban heat island, *Phys. Geogr.*, 2(1), 19–33,
575 doi:10.1080/02723646.1981.10642202, 1981.

576 Grimmond, C. S. B.: The suburban energy balance: Methodological considerations and results for a mid-latitude
577 west coast city under winter and spring conditions, *Int. J. Climatol.*, 12(5), 481–497,
578 doi:10.1002/joc.3370120506, 1992.

579 Heiple, S. and Sailor, D. J.: Using building energy simulation and geospatial modeling techniques to determine
580 high resolution building sector energy consumption profiles, *Energy Build.*, 40(8), 1426–1436,
581 doi:10.1016/j.enbuild.2008.01.005, 2008.

582 Hong, T., Ferrando, M., Luo, X. and Causone, F.: Modeling and analysis of heat emissions from buildings to
583 ambient air, *Appl. Energy*, 277(July), 115566, doi:10.1016/j.apenergy.2020.115566, 2020.

584 Iamarino, M., Beevers, S. and Grimmond, C. S. B.: High-resolution (space, time) anthropogenic heat emissions:
585 London 1970–2025, *Int. J. Climatol.*, 32(11), 1754–1767, doi:10.1002/joc.2390, 2012.

586 Ichinose, T., Shimodozono, K. and Hanaki, K.: Impact of anthropogenic heat on urban climate in Tokyo, *Atmos.*
587 *Environ.*, 33(24–25), 3897–3909 [online] Available from: [https://doi.org/10.1016/S1352-2310\(99\)00132-6](https://doi.org/10.1016/S1352-2310(99)00132-6),
588 1999.

589 Kelly, O. and Scott, P.: City vacant: Dublin’s hundreds of multimillion-euro empty sites and properties, [online]
590 Available from: [https://www.irishtimes.com/news/environment/city-vacant-dublin-s-hundreds-of-multimillion-](https://www.irishtimes.com/news/environment/city-vacant-dublin-s-hundreds-of-multimillion-euro-empty-sites-and-properties-1.3635595)
591 [euro-empty-sites-and-properties-1.3635595](https://www.irishtimes.com/news/environment/city-vacant-dublin-s-hundreds-of-multimillion-euro-empty-sites-and-properties-1.3635595), 2018.

592 Koralegedara, S. B., Lin, C. Y., Sheng, Y. F. and Kuo, C. H.: Estimation of anthropogenic heat emissions in
593 urban Taiwan and their spatial patterns, *Environ. Pollut.*, 215, 84–95, doi:10.1016/j.envpol.2016.04.055, 2016.

594 Lindberg, F., Grimmond, C. S. B., Yogeswaran, N., Kotthaus, S. and Allen, L.: Impact of city changes and
595 weather on anthropogenic heat flux in Europe 1995–2015, *Urban Clim.*, 4(2013), 1–15,

596 doi:10.1016/j.uclim.2013.03.002, 2013.

597 Nicol, J. F. and Humphreys, M. A.: Adaptive thermal comfort and sustainable thermal standards for buildings,
598 Energy Build., 34(6), 563–572, doi:10.1016/S0378-7788(02)00006-3, 2002.

599 Nie, W. S., Sun, T. and Ni, G. H.: Spatiotemporal characteristics of anthropogenic heat in an urban
600 environment: A case study of Tsinghua Campus, Build. Environ., 82, 675–686,
601 doi:10.1016/j.buildenv.2014.10.011, 2014.

602 Oikonomou, E., Davies, M., Mavrogianni, A., Biddulph, P., Wilkinson, P. and Kolokotroni, M.: Modelling the
603 relative importance of the urban heat island and the thermal quality of dwellings for overheating in London,
604 Build. Environ., 57(July 2006), 223–238, doi:10.1016/j.buildenv.2012.04.002, 2012.

605 Oke, T. R., Mills, G., Christen, A. and Voogt, J. A.: Urban Climates, Cambridge University Press., 2017.

606 Oliphant, A. J., Grimmond, C. S. B., Zutter, H. N., Schmid, H. P., Su, H. B., Scott, S. L., Offerle, B., Randolph,
607 J. C. and Ehman, J.: Heat storage and energy balance fluxes for a temperate deciduous forest, Agric. For.
608 Meteorol., 126(3–4), 185–201, doi:10.1016/j.agrformet.2004.07.003, 2004.

609 Sailor, D. J. and Lu, L.: A top-down methodology for developing diurnal and seasonal anthropogenic heating
610 profiles for urban areas, Atmos. Environ., 38(17), 2737–2748, doi:10.1016/j.atmosenv.2004.01.034, 2004.

611 Sailor, D. J. and Vasireddy, C.: Correcting aggregate energy consumption data to account for variability in local
612 weather, Environ. Model. Softw., 21(5), 733–738, doi:10.1016/j.envsoft.2005.08.001, 2006.

613 Santamouris, M., Papanikolaou, N., Livada, I., Koronakis, I., Georgakis, C., Argiriou, A. and Assimakopoulos,
614 D. N.: On the impact of urban climate on the energy consumption of building, Sol. Energy, 70(3), 201–216,
615 doi:10.1016/S0038-092X(00)00095-5, 2001.

616 Shepard, W.: Ghost cities of China: The story of cities without people in the world's most populated country,
617 Zed Books Ltd., 2015.

618 Takane, Y., Kikegawa, Y., Hara, M. and Grimmond, C. S. B.: Urban warming and future air-conditioning use in
619 an Asian megacity: importance of positive feedback, npj Clim. Atmos. Sci., 2(1), 1–11, doi:10.1038/s41612-
620 019-0096-2, 2019.

621 Wang, H. and Chen, Q.: A new empirical model for predicting single-sided, wind-driven natural ventilation in
622 buildings, Energy Build., 54, 386–394, doi:10.1016/j.enbuild.2012.07.028, 2012.

623 Wang, H. and Chen, Q.: A semi-empirical model for studying the impact of thermal mass and cost-return
624 analysis on mixed-mode ventilation in office buildings, Energy Build., 67, 267–274,
625 doi:10.1016/j.enbuild.2013.08.025, 2013.

626 Wang, K., Li, Y., Li, Y. and Lin, B.: Stone forest as a small-scale field model for the study of urban climate, *Int.*
627 *J. Climatol.*, 38(9), 3723–3731, doi:10.1002/joc.5536, 2018.

628 Wang, L. and Greenberg, S.: Window operation and impacts on building energy consumption, *Energy Build.*,
629 92, 313–321, doi:10.1016/j.enbuild.2015.01.060, 2015.

630 Warren, P.: Ventilation through openings on one wall only, in *Proceedings of International Centre for Heat and*
631 *Mass Transfer Seminar “Energy Conservation in Heating, Cooling, and Ventilating Buildings,”* Washington.,
632 1977.

633 Yu, Z., Hu, L., Sun, T., Albertson, J. and Li, Q.: Impact of heat storage on remote-sensing based quantification
634 of anthropogenic heat in urban environments, *Remote Sens. Environ.*, 262(May), 112520,
635 doi:10.1016/j.rse.2021.112520, 2021.

636